AEDC-TR-61-1

THEORETICAL LIGHT-GAS GUN PERFORMANCE

By

W. B. Stephenson

VKF, ARO, Inc.

May 1961

ARNOLD ENGINEERING DEVELOPMENT CENTER

AIR FORCE SYSTEMS COMMAND

US AF

THEORETICAL LIGHT-GAS GUN PERFORMANCE

By

W. B. Stephenson
VKF, ARO, Inc.

May 1961

AFSC Program Area 750A, Project No. 8950, Task 89600
ARO Project No. 386079

Contract No. AF 40(600)-800 S/A 11(60-110)

ABSTRACT

One-dimensional, unsteady flow theory of an ideal gas is reviewed as it applies to guns and ballistic model launchers. The method of characteristics is developed for the general case including chambrage and finite chamber volume. Results for helium as a propellant are given from which the required chamber size can be determined. The launch velocity for combinations of launch tube and chamber geometries is computed assuming no friction nor heat loss and an evacuated bore.

CONTENTS

ILLUSTRATIONS

NOMENCLATURE

A	Cross-section area
a	Acoustic speed
m	Mass
P	Pressure
S	Entropy
s	Distance
T	Temperature
t	Time
u	Velocity
u_o	Reference launch velocity ($A_1/A_2 = 1$, $x_{ch} \rightarrow \infty$)
V_c	Volume of chamber
V_L	Volume of launch tube
x_{ch}	Chamber length
γ	Ratio of specific heats
ρ	Density

SUBSCRIPTS

c	Chamber initial value	
ch	Conditions at end of chamber	
F	Forward face of piston	
L	Sonic exit limit; launch tube	
o	Standard	
p	Piston or projectile	
R	Rear face of piston	
t, s	Partial derivatives	
1	Upstream of chamber exit	Flow from chamber
2	Downstream of chamber exit	Flow from chamber

1	Ahead of incident shock	Normal shocks
2	Behind incident shock	
3	Behind first reflected shock	
4	Behind first shock reflected from piston face	

DIMENSIONLESS COORDINATES

$\bar{s}$ $\quad \dfrac{P_c A_L}{m_M a_c^2} s$

$\bar{t}$ $\quad \dfrac{P_c A_L}{m_M a_c} t$

$\bar{u}$ $\quad u/a_c$

$\bar{a}$ $\quad a/a_c$

$\bar{P}$ $\quad P/P_c$

P_c, a_c Initial chamber conditions

m_M Projectile mass

INTRODUCTION

The light-gas gun type of ballistic model launcher has made it possible to simulate flight environment at very high speeds more closely than by any other ground experimental facility. A light gas (hydrogen or helium) is necessary as a propellant because the associated high acoustic speed allows the chamber pressure to be transmitted to the projectile base with lesser decrease at high speeds than when a heavier propellant is used.

The highest velocities have been achieved with launchers in which the propellant light gas is raised to a final high energy state by compression with a free piston. Velocities in the range between 25,000 and 30,000 ft/sec are regularly obtained using light projectiles.

One of the important aspects of the design of launchers is the effect of geometrical variables of the configuration on the performance. The launch tube length, chamber length, and chambrage (chamber cross-section to launch tube cross-section area ratio) are the essential dimensions. The calculation of the unsteady flow in one dimension by the method of characteristics appeared to be the most practicable approach to the problem. Reference 1 provides a general background for the analysis, and Seigal (Ref. 2) treats the effect of chambrage for infinitely long chambers. The effect of finite chamber length is considered by Heybey (Ref. 3) for a launch tube the same diameter as the chamber. Calculations for ratios of specific heats, γ, of 1.25 and 1.4 are shown in Ref. 2, and the method of calculation is given in Ref. 3. It was considered most desirable to make the characteristics calculations for finite chamber volume, chambrage, and $\gamma = 1.66$ corresponding to helium in order to have useful results for light-gas launchers that can be verified experimentally. In a two-stage configuration, the volume after compression is likely to become very small, and it varies widely with operating conditions. It is therefore obvious that the compression tube must be properly matched to the launch tube to obtain the optimum performance of the system. The general characteristics solutions provide the information required for finding the minimum chamber for a fixed launch tube.

The characteristics results provide a starting point for estimating the effect of heat losses from the propellant. Since the method is a step-by-step process, it lends itself readily to the introduction of projectile friction, real gas properties, and relaxation times.

Manuscript released by author February 1961.

UNSTEADY, ISENTROPIC PROCESSES IN ONE-DIMENSIONAL FLOW

GENERAL RELATIONS

The concept of one-dimensional flow treated here corresponds to the motion of a gas in a constant area tube in which the properties are uniform across any section. No heat is transferred across the tube walls, and viscosity is neglected.

Basic equations for one-dimensional flow of an ideal gas are:

Conservation of Mass: $\frac{\partial \rho}{\partial t} + \frac{\partial(\rho u)}{\partial s} = 0$

Conservation of Momentum: $\frac{\partial(\rho u)}{\partial t} + \frac{\partial(\rho u^2)}{\partial s} + \frac{\partial P}{\partial s} = 0$

Isentropic Flow: $\frac{\partial S}{\partial t} + u \frac{\partial S}{\partial s} = 0$

The last condition, with initially uniform conditions and the equation of state, implies the following isentropic relations between the gas properties:

$$\left(\frac{T}{T_o}\right)^{1/2} = \left(\frac{\rho}{\rho_o}\right)^{\frac{(\gamma-1)}{2}} = \left(\frac{P}{P_o}\right)^{\frac{(\gamma-1)}{2\gamma}}$$

The speed of sound is found to be

$$a^2 = \frac{dP}{d\rho} = \gamma \frac{P}{\rho}$$

and can be expressed as

$$\frac{a}{a_o} = \left(\frac{T}{T_o}\right)^{1/2}$$

Rewriting the continuity equation

$$\rho_t + \rho u_s + u \rho_s = 0$$

or by introducing the acoustic speed,

$$P_t + u P_s + \rho a^2 u_s = 0$$

which, by adding and subtracting from the momentum equation:

$$\rho u_t + \rho u u_s + P_s = 0$$

yields two equations for unsteady, isentropic, one-dimensional flow:

$$P_t + (u + a) P_s + \rho a \left[u_t + (u + a) u_s\right] = 0$$

and

$$P_t + (u - a) P_s - \rho a \left[u_t + (u - a) u_s\right] = 0$$

These relations are most clearly understood by considering the "wave plane" or $s - t$ plane. By defining two directions in this plane:

$$\left.\frac{ds}{dt}\right) = u + a$$

and

$$\left.\frac{ds}{dt}\right) = u - a$$

the flow properties along these lines are related by

$$dP = -\rho a\, du$$

and

$$dP = +\rho a\, du$$

Integration of these with the aid of the isentropic relations provides the following:

$$\left(\frac{\gamma - 1}{2}\right) u + a = \text{const. corresponds to } \frac{ds}{dt} = u + a$$

and

$$\left(\frac{\gamma - 1}{2}\right) u - a = \text{const. corresponds to } \frac{ds}{dt} = u - a$$

The two directions, $u + a$ and $u - a$, on the s-t plane are evidently the paths of sound waves traveling respectively downstream and upstream through a tube in which the flow velocity is u. The lines having slopes $u + a$ and $u - a$ are termed downstream and upstream characteristics. If the velocity u and speed of sound a are known at a point on a characteristic, then the relationship between u and a is known at all points along it.

APPLICATION TO PISTON MOTION

It is instructive to find the motion of a frictionless piston in an infinite tube of cross section A having the initial conditions: (1) the piston of mass m is at rest; (2) the acoustic speed behind the piston is a; and (3) the tube is evacuated ahead of the piston.

The $s - t$ plane appears as:

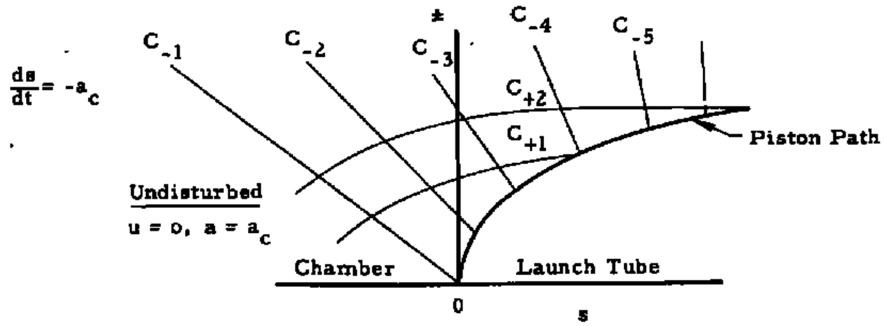

An unsteady flow region develops behind the piston bounded by a sound wave and the piston path. In this region the downstream characteristics, C_+, connect the undisturbed region with the piston and have the property

$$\frac{\gamma - 1}{2} u + a = a_c$$

It is evident that the first upstream characteristic, C_{-1}, is linear, since along it $u = 0$ and $a = a_c$ and $ds/dt = -a_c$. By considering the piston motion to consist of straight segments having discontinuous changes in slope, it can be seen that an upstream characteristic fan is generated by rays starting at each discontinuity. The left-hand edge of this fan is a straight line by the same reasoning as above -- it bounds a region of constant velocity and sound speed. In the limit of an infinitesimal slope change, the fan reduces to a single characteristic line which is straight. Thus, the simple wave region behind the piston is characterized by straight diverging characteristics, C_-, having the slope

$$\frac{ds}{dt} = u_p - a_p = - a_c + \frac{\gamma - 1}{2} u_p$$

The downstream characteristics, C_+, on the other hand, are curved and have the slope

$$\frac{ds}{dt} = u_p + a_p = a_c + \left(\frac{3 - \gamma}{2}\right) u_p$$

at their intersections with the straight characteristics.

The above is the model of an idealized gun having an effectively infinite chamber with the same bore as the barrel. The acceleration of the piston is

$$\frac{du_p}{dt} = u_p \frac{du_p}{ds} = \frac{PA}{m}$$

Then, since the characteristics that arrive at the rear of the piston are connected to a state of known properties indicated by the subscript (c), the following relation holds:

$$\left(\frac{\gamma - 1}{2}\right) u_p + a_p = a_c$$

and through the isentropic relationship

$$\frac{P_p}{P_c} = \left(\frac{a_p}{a_c}\right)^{\frac{2\gamma}{\gamma - 1}} = \left[1 - \left(\frac{\gamma - 1}{2}\right) \frac{u_p}{a_c}\right]^{\frac{2\gamma}{\gamma - 1}}$$

the acceleration becomes

$$u_p \frac{du_p}{ds} = \frac{P_c A}{m}\left[1 - \left(\frac{\gamma - 1}{2}\right) \frac{u_p}{a_c}\right]^{\frac{2\gamma}{\gamma - 1}}$$

which can be integrated to yield the velocity distance function:

$$\frac{P_c A}{m} s = \int_0^{u_p} u_p \left[1 - \left(\frac{\gamma - 1}{2}\right) \frac{u_p}{a_c}\right]^{-\frac{2\gamma}{\gamma - 1}} du_p$$

It is usual to express this in the dimensionless form,

$$\frac{P_c A}{m a_c^2} s = \int_0^{\frac{u_p}{a_c}} \frac{u_p}{a_c} \left[1 - \left(\frac{\gamma - 1}{2}\right) \frac{u_p}{a_c}\right]^{-\frac{2\gamma}{\gamma - 1}} \frac{du_p}{a_c}$$

which can be integrated (Ref. 5) to yield

$$\bar{s} = \frac{2}{\gamma - 1} \left[\frac{\frac{2}{\gamma + 1} - \left(1 - \frac{\gamma - 1}{2} \bar{u}_p\right)}{\left(1 - \frac{\gamma - 1}{2} \bar{u}_p\right)^{\frac{\gamma + 1}{\gamma - 1}}} + \frac{\gamma - 1}{\gamma + 1} \right]$$

where

$$\bar{s} = \frac{P_c A s}{m a_c^2}$$

and

$$\bar{u}_p = \frac{u_p}{a_c}$$

Similarly, letting $\bar{t} = \frac{P_c A}{m a_c} t$

$$\bar{t} = \int_0^{\bar{u}_p} \frac{d\bar{u}_p}{\left[1 - \left(\frac{\gamma - 1}{2}\right) \bar{u}_p\right]^{\frac{2\gamma}{\gamma - 1}}} = \frac{\frac{2}{\gamma + 1}}{\left[1 - \left(\frac{\gamma - 1}{2}\right) \bar{u}_p\right]^{\frac{\gamma + 1}{\gamma - 1}}} - \frac{2}{\gamma + 1}$$

These general relations are shown in Fig. 2.

When the launch tube is infinitely long or when the projectile weight approaches zero (contact discontinuity), the velocity becomes $\frac{2}{\gamma - 1}$.

The velocity of the unchambered gun having an infinitely long chamber provides a convenient reference performance for comparison with more realistic models to be discussed.

The effect of chambrage is discussed in detail in a later section; however, as a first approximation to the effect of chambrage, several authors (Ref. 4) consider the chamber to be an infinite reservoir from which critical flow is established immediately upon projectile motion. The energy equation gives for the exit flow:

$$a_2^2 + \left(\frac{\gamma - 1}{2}\right) u_2^2 = a_c^2 \qquad\qquad \frac{A_1}{A_2} \rightarrow \infty$$

and since

$$u_2 = a_2$$

$$u_2 = \sqrt{\frac{2}{\gamma + 1}}\, a_c$$

from which the downstream characteristic value is given by:

$$a + \left(\frac{\gamma - 1}{2}\right) u = a_2 + \left(\frac{\gamma - 1}{2}\right) u_2 = \sqrt{\frac{\gamma + 1}{2}}\, a_c$$

or in a non-dimensional form:

$$\bar{a} + \left(\frac{\gamma - 1}{2}\right) \bar{u} = \sqrt{\frac{\gamma + 1}{2}}$$

so that

$$\bar{a}_p = \sqrt{\frac{\gamma + 1}{2}} - \left(\frac{\gamma - 1}{2}\right) \bar{u}_p$$

and

$$\bar{P}_R = \left[\sqrt{\frac{\gamma + 1}{2}} - \left(\frac{\gamma - 1}{2}\right) \bar{u}_p\right]^{\frac{2\gamma}{\gamma - 1}} \qquad \text{(See Fig. 1)}$$

Obviously, this pressure can never be greater than 1.0 and the actual pressure is approximately as shown by the dashed curve in Fig. 1. A reasonably good approximation to the velocity is obtained by assuming that the exit pressure given by the steady energy equation acts on the projectile base up to the point where the exit flow is sonic.

SHOCK COMPRESSION AHEAD OF A PISTON AND FORWARD FACE PRESSURE

PISTON FORWARD FACE PRESSURE

Free piston applications of the gun principle utilize a compression tube that is charged with an initial pressure (P_1). The forward face pressure on the piston (P_F) is derived in a quasi-steady manner assuming it is the pressure behind a steady normal shock. The pressure ratio across the shock is given in terms of piston velocity (Ref. 1):

$$\frac{P_2}{P_1} = 1 + \left(\frac{\gamma}{2}\right) \frac{u_p}{a_1} \left[\frac{\gamma + 1}{2}\, \frac{u_p}{a_1} + \sqrt{4 + \left(\frac{\gamma + 1}{2}\, \frac{u_p}{a_1}\right)^2}\,\right] = \frac{P_F}{P_1}$$

Referring the pressures and velocities to chamber conditions P_c and a_c:

$$\frac{\bar{P}_F}{\bar{P}_1} = 1 + \left(\frac{\gamma}{2}\right) \frac{\bar{u}_p}{\bar{a}_1} \left[\frac{\gamma+1}{2} \frac{\bar{u}_p}{\bar{a}_1} + \sqrt{4 + \left(\frac{\gamma+1}{2} \frac{\bar{u}_p}{\bar{a}_1}\right)^2}\right]$$

$$\bar{u} = \frac{u_p}{a_c}$$

$$\bar{a} = \frac{a}{a_c}$$

$$\bar{P} = \frac{P}{P_c}$$

Figure 3 shows forward face pressure as it varies with piston velocity for a range of acoustic speed ratios, $\bar{a}_1$.

The piston speed may be computed from:

$$\bar{s} = \int_0^{\bar{u}} \frac{\bar{u}\, d\bar{u}}{\bar{P}_R - \bar{P}_F}$$

for various $\bar{P}_1$ and the appropriate γ_c, γ_1, and $\bar{a}_1$.

SHOCK COMPRESSION IN A PUMP TUBE

When gas is driven ahead of a relatively fast moving piston, a shock wave runs ahead of it. The pressure ratio across this wave is related to the piston velocity by:

$$\left(\frac{u_p}{a_1}\right)^2 = \frac{2}{\gamma_1(\gamma_1+1)} \frac{\left(\frac{P_2}{P_1} - 1\right)^2}{\frac{P_2}{P_1} + \frac{\gamma_1 - 1}{\gamma_1 + 1}}$$

The density and temperature ratios are given by:

$$\frac{\rho_2}{\rho_1} = \frac{\frac{P_2}{P_1} + \frac{\gamma_1 - 1}{\gamma_1 + 1}}{1 + \left(\frac{\gamma_1 - 1}{\gamma_1 + 1}\right) \frac{P_2}{P_1}}$$

and

$$\frac{T_2}{T_1} = \left(\frac{a_2}{a_1}\right)^2 = \frac{\frac{P_2}{P_1}}{\frac{\rho_2}{\rho_1}}$$

These functions are shown in Fig. 4 for $\gamma = 1.66$

If the end of the piston tube is closed, the shock will reflect leaving a state (3) of high pressure and temperature and zero velocity relative to the tube. This reflected shock will then reflect again from the piston face which is assumed to be traveling at its original speed, resulting in the conditions (4) (Fig. 5). If the piston is infinitely massive, shocks will continue to be reflected from the piston and end of the compression tube. These shocks have in common the velocity change across the shock equal to the piston speed, u_p. However, since the sonic speed ahead of each shock is continuously increasing, the shock Mach number becomes progressively smaller. The shock compression approaches an isentropic process, and the difference between shock and isentropic compression after the first three shock transits is small. Figure 6a shows this in the comparison of the pressure-temperature relation for six shock transits compared to three transits followed by an isentropic compression to the same pressure. This leads to the conclusion that if the final pressure in this type of compression tube can be determined (empirically or otherwise), the final state of compressed gas will be known. Practically, the final temperature may then be related to that for isentropic compression by:

$$\frac{T_f}{T_{isen}} = \frac{\left(\frac{T_f}{T_4}\right)\left(\frac{T_4}{T_1}\right)}{\left(\frac{P_f}{P_1}\right)^{\frac{\gamma-1}{\gamma}}} = \frac{\left(\frac{P_f}{P_4}\right)^{\frac{\gamma-1}{\gamma}}}{\left(\frac{P_f}{P_1}\right)^{\frac{\gamma-1}{\gamma}}}\,\frac{T_4}{T_1} = \frac{\frac{T_4}{T_1}}{\left(\frac{P_4}{P_1}\right)^{\frac{\gamma-1}{\gamma}}} \quad \text{(see Fig. 6b)}$$

This system of heating of a gas has application to launcher systems of the two-stage free piston type.

EFFECT OF CHAMBRAGE

Chambrage will be defined as the ratio of chamber to launch tube cross-section areas. The transition is assumed to be very short, and with increasing time the flow will approach sonic velocity at the exit. Following Seigal (Ref. 2) the assumptions below are made.

1. Flow in the chamber is unsteady isentropic.
2. Quasi-steady conservation equations apply through the transition.
3. The characteristics originate from a rest state defined by the acoustic velocity, a_{ch}, at the end of the chamber.

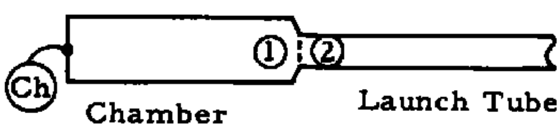

Then, the following equations apply:

Unsteady, one-dimensional flow in chamber --

$$a_{ch} = a_1 + \left(\frac{\gamma - 1}{2}\right) u_1$$

Continuity through the transition --

$$\frac{u_1}{u_2} = \left(\frac{A_2}{A_1}\right)\left(\frac{\rho_2}{\rho_1}\right) = \left(\frac{A_2}{A_1}\right)\left(\frac{a_2}{a_1}\right)^{\frac{2}{\gamma - 1}}$$

Energy equation through the transition --

$$u_1^2 + \left(\frac{2}{\gamma - 1}\right) a_1^2 = u_2^2 + \left(\frac{2}{\gamma - 1}\right) a_2^2$$

The above reduce to the following relations between the quantities, u_1, a_1, u_2, and a_2:

$$\frac{a_{ch}}{a_1} = 1 + \sqrt{\frac{1 - \left(\frac{a_2}{a_1}\right)^2}{\left(\frac{2}{\gamma - 1}\right)\left[\left(\frac{A_1}{A_2}\right)^2 \left(\frac{a_1}{a_2}\right)^{\frac{4}{\gamma - 1}} - 1\right]}}$$

$$\frac{u_1}{u_2} = \left(\frac{A_2}{A_1}\right)\left(\frac{a_2}{a_1}\right)^{\frac{2}{\gamma - 1}}$$

and

$$\frac{u_1}{a_{ch}} = \left(\frac{2}{\gamma - 1}\right)\left(1 - \frac{a_1}{a_{ch}}\right)$$

The relations between characteristic values, $\left(\frac{\gamma - 1}{2}\right) u \pm a$, and characteristic slopes, $u \pm a$, across the transition section ① and ② can be determined. The generality of the relationships is increased by dividing all the velocities by a_{ch} and further normalizing with the initial undisturbed acoustic velocity, a_c, ($a_{ch} = a_c$ until the first upstream characteristic arrives at the end of the chamber). For use in characteristics calculations the following functions are most useful:

Upstream characteristics from chamber exit into chamber

$$\left(\frac{\gamma - 1}{2}\right)\left(\frac{\bar{u}_1}{\bar{a}_{ch}}\right) - \left(\frac{\bar{a}_1}{\bar{a}_{ch}}\right)$$

where

$$\bar{u} = \frac{u}{a_c} \quad \text{and} \quad \bar{a}_{ch} = \frac{a_{ch}}{a_c}$$

Downstream characteristics from chamber exit into launch tube

$$\left(\frac{\gamma-1}{2}\right)\left(\frac{\bar{u}_2}{\bar{a}_{ch}}\right)+\left(\frac{\bar{a}_2}{\bar{a}_{ch}}\right)$$

The chamber exit velocities

$$\frac{\bar{u}_1}{\bar{a}_{ch}}\,,\ \frac{\bar{a}_1}{\bar{a}_{ch}}\,,\ \frac{\bar{u}_2}{\bar{a}_{ch}}\,,\ \text{and}\ \frac{\bar{a}_2}{\bar{a}_{ch}}$$

as functions of the upstream characteristic value from the projectile path to the chamber exit,

$$\left(\frac{\gamma-1}{2}\right)\frac{\bar{u}_2}{\bar{a}_{ch}}-\frac{\bar{a}_2}{\bar{a}_{ch}}=\left(\frac{\gamma-1}{2}\right)\frac{\bar{u}_p}{\bar{a}_{ch}}-\frac{\bar{a}_p}{\bar{a}_{ch}}$$

Graphs of these functions, (Figs. 7a, b, c, and d) permit determination of the change in the characteristics as they cross the chamber exit. Flow from the chamber is limited by sonic conditions at the exit, i. e., $u_1 = a_2$. Setting this limit and solving the preceeding equations, the limit chamber exit acoustic velocity, a_{1_L}, is given by:

$$\frac{A_1}{A_2}=\frac{\gamma-1}{2\left(\frac{a_{ch}}{a_{1_L}}-1\right)}\left\{\left(\frac{2}{\gamma+1}\right)\left[1+\left(\frac{2}{\gamma-1}\right)\left(\frac{a_{ch}}{a_{1_L}}-1\right)^2\right]\right\}^{\frac{\gamma+1}{2(\gamma-1)}}$$

from which the remaining velocities, u_{1_L}, u_{2_L}, and a_{2_L}, are determined.

The effect of chambrage on projectile velocity is illustrated in the way the limit of the downstream characteristic value $\left(\frac{\gamma-1}{2}\bar{u}_2+\bar{a}_2\right)$ varies with area ratio, $\frac{A_1}{A_2}$. If the chamber is infinitely long, $\bar{a}_{ch}=1$; then the ultimate velocity is given by the condition that $\bar{a}_p = 0$

$$\left(\frac{\gamma-1}{2}\right)\bar{u}_p+\bar{a}_p=\left(\frac{\gamma-1}{2}\right)\bar{u}_2+\bar{a}_2$$

$$\bar{u}_{max}=\left(\frac{2}{\gamma-1}\right)\left[\left(\frac{\gamma-1}{2}\right)\bar{u}_{2_L}+\bar{a}_{2_L}\right]$$

If there is no chambrage

$$u_{max}=\left(\frac{2}{\gamma-1}\right)a_c=3.03\,a_c\qquad(\gamma=1.66)$$

Compared to

$$u_{max}=1.1\left(\frac{2}{\gamma-1}\right)a_c=3.33\,a_c\qquad(\gamma=1.66)\quad\text{(Fig. 7a)}$$

or about 10 percent increase for $\frac{A_1}{A_2}=4$.

When the chamber has a finite length, $\bar{a}_{ch}$ is 1.0 until the first reflected characteristic reaches the exit after which time it drops with the pressure at the breech end of the chamber.

GENERAL CHARACTERISTICS SOLUTION FOR CHAMBERED GUNS

STARTING POINT – INITIAL POINT ON THE PROJECTILE PATH

In the early stages of projectile motion, its velocity is small, and the pressure acting on its base may be assumed equal to that at the chamber exit. In the following, the launch tube ahead of the projectile is assumed evacuated. Figure 7c shows the relation between $\bar{a}_2$ and $\bar{u}_2$ since $\bar{a}_c = 1$ at the early time points. Graphical integration yields the coordinates of the first point:

$$\bar{s}_p = \int_0^{\bar{u}_p} \frac{\bar{u}_p \, d\,\bar{u}_p}{\bar{P}_2} = \int_0^{\bar{u}} \frac{\bar{u}_p \, d\,\bar{u}_p}{(\bar{a}_2)^{\frac{2\gamma}{\gamma - 1}}}$$

$$\bar{t}_p = \int_0^{\bar{u}_p} \frac{d\,\bar{u}_p}{\bar{P}_2} = \int_0^{\bar{u}_p} \frac{d\,\bar{u}_p}{(\bar{a}_2)^{\frac{2\gamma}{\gamma - 1}}}$$

Numerical computations indicate that the assumption, $\bar{a}_2 = \bar{a}_p$, introduces negligible error for $\bar{u}_p \leq 0.3$. Beyond this point, characteristics methods of the following sections are used.

Since $\bar{u}$ and $\bar{a}$ are practically constant between the projectile and exit, the upstream characteristic is a straight line with the slope, $\bar{u}_p - \bar{a}_p$.

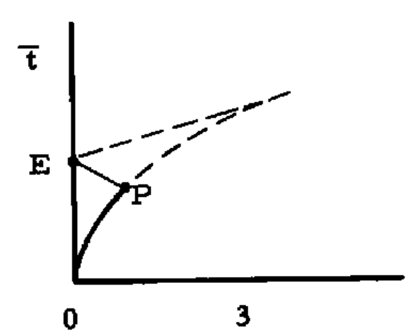

At the exit point, E :

$$\bar{S}_E = 0$$

$$\bar{t}_E = \frac{\bar{S}_p}{\bar{u}_p - \bar{a}_p} + \bar{t}_p$$

$$\bar{u}_E = \bar{u}_p \text{ and } \bar{a}_E = \bar{a}_p$$

GENERAL NET INTERSECTION POINT

In building up the characteristics network, new point, C, will be required, which lies at the intersection of a downstream characteristic from point, A, and an upstream characteristic from point, B.

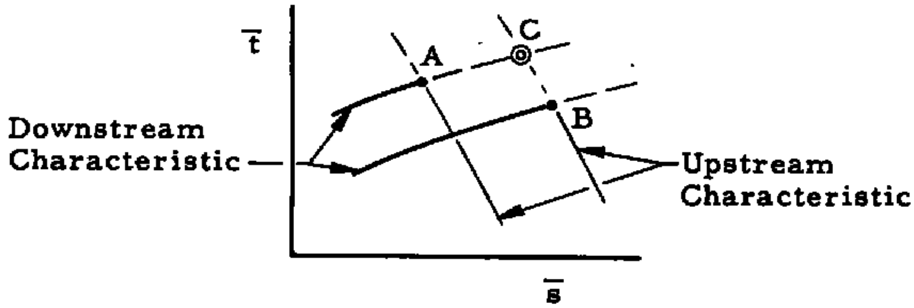

At C, $\left(\frac{\gamma-1}{2}\right) \bar{u}_C + \bar{a}_C = \left(\frac{\gamma-1}{2}\right) \bar{u}_C + \bar{a}_A$

$$\left(\frac{\gamma-1}{2}\right) \bar{u}_C - \bar{a}_C = \left(\frac{\gamma-1}{2}\right) \bar{u}_B - \bar{a}_B$$

and the local slopes are

$\bar{u}_C + \bar{a}_C$ corresponding to the downstream characteristic

$\bar{u}_C - \bar{a}_C$ corresponding to the upstream characteristic

The first two equations are solved for $\bar{u}_C$ and $\bar{a}_C$:

$$\bar{a}_C = \frac{1}{2}\left[\left(\frac{\gamma-1}{2}\right) \bar{u}_A + \bar{a}_A - \left(\frac{\gamma-1}{2}\right) \bar{u}_B - \bar{a}_B\right]$$

$$\bar{u}_C = \frac{2}{\gamma-1}\left[\left(\frac{\gamma-1}{2}\right) \bar{u}_A + \bar{a}_A - \bar{a}_C\right]$$

The coordinates of the point, C, are determined by extending the downstream characteristic at the mean slope

$$\frac{1}{2}(\bar{u}_A + \bar{a}_A + \bar{u}_C + \bar{a}_C)$$

and the upstream characteristic at the mean slope

$$\frac{1}{2}(\bar{u}_B - \bar{a}_B + \bar{u}_C - \bar{a}_C).$$

Solving the following equations simultaneously:

$$\bar{s}_C - \bar{s}_A = \frac{1}{2}(\bar{u}_A + \bar{a}_A + \bar{u}_C + \bar{a}_C)(\bar{t}_C - \bar{t}_A)$$

and

$$\bar{s}_C - \bar{s}_B = \frac{1}{2}(\bar{u}_B - \bar{a}_B + \bar{u}_C - \bar{a}_C)(\bar{t}_C - \bar{t}_B)$$

The coordinates in the $\bar{s} - \bar{t}$ plane are found to be:

$$\bar{t}_C = \frac{2(\bar{s}_B - \bar{s}_A) + \bar{t}_A(\bar{u}_A + \bar{a}_A + \bar{u}_C + \bar{a}_C) - \bar{t}_B(\bar{u}_B - \bar{a}_B + \bar{u}_C - \bar{a}_C)}{\bar{u}_A + \bar{a}_A + 2\bar{a}_C - (\bar{u}_B - \bar{a}_B)}$$

and

$$\bar{s}_C = \bar{s}_A + \frac{1}{2}(\bar{u}_A + \bar{a}_A + \bar{u}_C + \bar{a}_C)(\bar{t}_C - \bar{t}_A)$$

POINTS ON THE PROJECTILE PATH

In this case, a point, A, on a downstream characteristic and a preceding point, B, on the projectile path will be known. The next point, C, on the

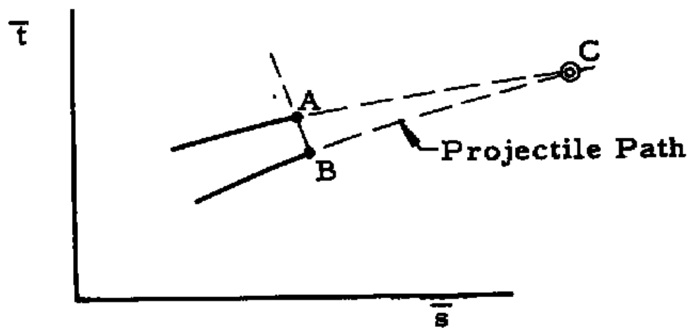

projectile path is to be determined. A method of successive approximations must be adopted (Ref. 3). For the general nth approximation, the mean slopes of the characteristic and the projectile path are given by:

$$\left(\frac{d\bar{s}}{d\bar{t}}\right)_+ = \alpha(n) = \frac{1}{2}\left[\bar{u}_A + \bar{a}_A + \bar{u}_C(n-1) + \bar{a}_C(n-1)\right]$$

$$\left(\frac{d\bar{s}}{d\bar{t}}\right)_p = \beta(n) = \frac{1}{2}\left[\bar{u}_B + \bar{u}_C(n-1)\right]$$

The corresponding approximate coordinate and velocities are given by:

$$\bar{t}_C(n) = \frac{\bar{s}_B - \bar{s}_A + \alpha(n)\bar{t}_A - \beta(n)\bar{t}_B}{\alpha(n) - \beta(n)}$$

$$\bar{u}_C(n) = \bar{u}_B + \frac{1}{2}\left\{(\bar{a}_B)^{\frac{2\gamma}{\gamma-1}} + \left[\bar{a}_C(n-1)\right]^{\frac{2\gamma}{\gamma-1}}\right\}\left[\bar{t}_C(n) - \bar{t}_B\right]$$

$$\bar{a}_c(n) = \bar{a}_A + \left(\frac{\gamma-1}{2}\right)\left[\bar{u}_A - \bar{u}_C(n)\right]$$

The first approximation is made by assuming the slopes at C are the same as at A and B. That is

$$\alpha\ (1) = \bar{u}_A + \bar{a}_A$$

$$\beta\ (1) = \bar{u}_B$$

$$\bar{t}_C\ (1) = \frac{\bar{s}_B - \bar{s}_A + (\bar{u}_A + \bar{a}_A)\,\bar{t}_A - \bar{u}_B\,\bar{t}_B}{\bar{u}_A + \bar{a}_A - \bar{u}_B}$$

$$\bar{u}_C\ (1) = \bar{u}_B + (\bar{a}_B)^{\frac{2\gamma}{\gamma - 1}} \left[\bar{t}_C\ (1) - \bar{t}_B\right]$$

$$\bar{a}_C\ (1) = \bar{a}_A + \left(\frac{\gamma - 1}{2}\right) \left[\bar{u}_A - \bar{u}_C\ (1)\right]$$

This system converges satisfactorily in three to five steps and permits calculation of the remaining coordinate, $\bar{s}_C$:

$$\bar{s}_C = \bar{s}_B + \frac{1}{2}\,(\bar{u}_B + \bar{u}_C)(\bar{t}_C - \bar{t}_B)$$

POINTS AT THE BREECH END OF CHAMBER

The velocity, $\bar{u}$, vanishes at the wall resulting in the following:

$\bar{a}_{ch}$ = Downstream characteristic value and slope, $d\bar{s}/d\bar{t}$

$-\bar{a}_{ch}$ = Upstream characteristic value and slope

A point, A, will be known in an upstream characteristic having the value

$$\left(\frac{\gamma - 1}{2}\right) \bar{u} - \bar{a} = \left(\frac{\gamma - 1}{2}\right) \bar{u}_A - \bar{a}_A$$

then and the point, B, of the breech end will be given by:

$$-\bar{a}_B = \left(\frac{\gamma - 1}{2}\right) \bar{u}_A - \bar{a}_A$$

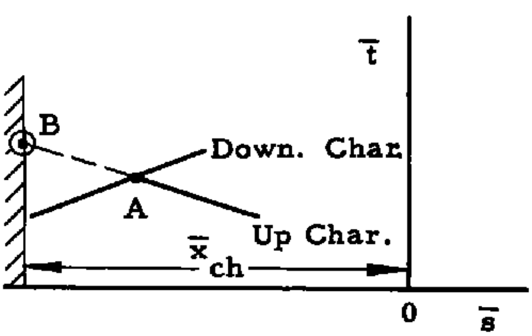

$$\bar{s}_B = -\bar{X}_{ch}$$

$$\bar{t}_B = \bar{t}_A - \frac{2\,(\bar{X}_{ch} - \bar{s}_A)}{\bar{u}_A - \bar{a}_A - \bar{a}_B}$$

$$\bar{u}_B = 0$$

PROCEDURE FOR DETERMINING FLOW THROUGH THE EXIT

In general a point, A, on the downstream characteristic in the chamber and a downstream characteristic, a, b, c, d, in the launch tube are known. This is illustrated below:

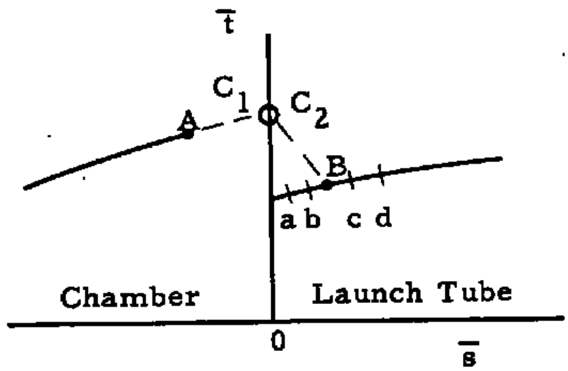

At the unknown point, C, C_1 corresponds to the conditions upstream and C_2 downstream at the chamber exit. Since the point, B, is not known, it will be necessary to use a graphical method. A series of values for $\bar{u}_1$ at C are assumed slightly greater than $\bar{u}_A$ from which corresponding times, $\bar{t}_C$, are determined:

(1) $$\bar{t}_C = \bar{t}_A - \frac{2\,\bar{s}_A}{\bar{u}_A + \bar{a}_A + \bar{u}_C + \bar{a}_C}$$

(2) Determine the upstream characteristic $\left(\frac{\gamma-1}{2}\right)\bar{u}_2 - \bar{a}_2$ from Figs. 7a and d. $\frac{\bar{u}_1}{\bar{a}_{ch}}$ is a function of $\left(\frac{\gamma-1}{2}\right)\frac{\bar{u}_2}{\bar{a}_{ch}} - \frac{\bar{a}_2}{\bar{a}_{ch}}$ as is $\left(\frac{\gamma-1}{2}\right)\frac{\bar{u}_2}{\bar{a}_{ch}} + \frac{\bar{a}_2}{\bar{a}_{ch}}$. Multiply by $\bar{a}_{ch}$ to obtain $\left(\frac{\gamma-1}{2}\right)\bar{u}_2 - \bar{a}_2$ and $\left(\frac{\gamma-1}{2}\right)\bar{u}_2 + \bar{a}_2$; solve for $\bar{u}_2$ and $\bar{a}_2$.

(3) On the $\bar{t} - \bar{s}$ plane, upstream characteristics arriving at C are shown below:

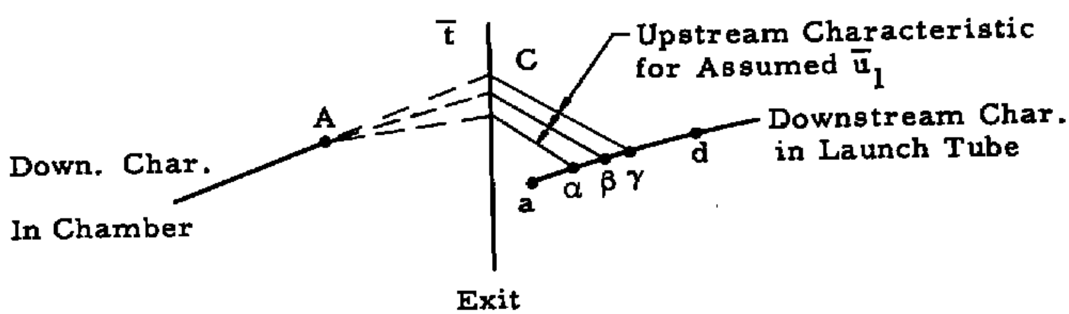

The slopes of upstream characteristics will be $\frac{1}{2}(\bar{u}_2 - \bar{a}_2 + \bar{u} - \bar{a})$ where $\bar{u}$ and $\bar{a}$ are determined at the intersection with the downstream characteristic, a, b, c, d. Along this characteristic $\left(\frac{\gamma - 1}{2}\right)\bar{u} + \bar{a} = \text{const.} = \left(\frac{\gamma - 1}{2}\right)\bar{u}_a + \bar{a}_a$, and for the assumed upstream characteristics $\left(\frac{\gamma - 1}{2}\right)\bar{u} - \bar{a} = \text{const.} = \left(\frac{\gamma - 1}{2}\right)\bar{u}_2 - \bar{a}_2$. $\bar{u}$ and $\bar{a}$ at the intersections, α, β, and γ, of the characteristics may now be solved for by adding and subtracting the two simultaneous equations.

(4) Plot upstream characteristic value $\left(\frac{\gamma - 1}{2}\right)\bar{u} - \bar{a}$ vs $\bar{s}$ for the intersection points above and for the known points, a, b, c, d, along the known downstream characteristic:

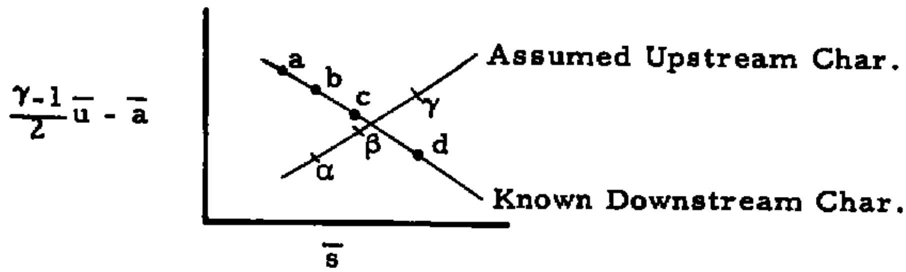

At the intersection read $\left(\frac{\gamma - 1}{2}\right)\bar{u}_2 - \bar{a}_2$; from $\left(\frac{\gamma - 1}{2}\right)\frac{\bar{u}_2}{\bar{a}_{ch}} - \frac{\bar{a}_2}{\bar{a}_{ch}}$, find $\frac{\bar{u}_1}{\bar{a}_C}$ from Fig. 7d; compute $\bar{u}_1$, $\bar{a}_1 = \bar{a}_{ch} - \left(\frac{\gamma - 1}{2}\right)\bar{u}_1$, and $\bar{t}_C$ as was done for the assumed values of $\bar{u}_1$.

(5) From Fig. 7a find $\left(\frac{\gamma - 1}{2}\right)\frac{\bar{u}_2}{\bar{a}_{ch}} + \frac{\bar{a}_2}{\bar{a}_{ch}}$ and compute $\left(\frac{\gamma - 1}{2}\right)\bar{u}_2 + \bar{a}_2$. $\bar{u}_2$ and $\bar{a}_2$ are then determined at the point, C, on the downstream chamber exit characteristic.

Flow through Exit Prior to Arrival of First Reflected Characteristic (or the Special Case of the Infinitely Long Chamber)

Until the first reflected characteristic reaches the chamber exit, the chamber downstream characteristic value $\left(\frac{\gamma - 1}{2}\right)\bar{u} + \bar{a} = 1 = \bar{a}_{ch}$. The procedure is considerably simplified because the solution is obtained directly from Fig. 7a without successive trials. A point, B, will be known at which the upstream characteristic, $\left(\frac{\gamma-1}{2}\right)\bar{u}_B - \bar{a}_B$, has been determined.

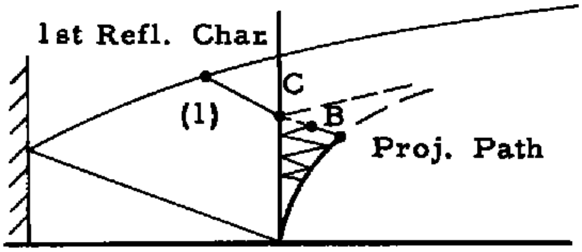

The value of $\left(\frac{\gamma-1}{2}\right)\bar{u}_2 - \bar{a}_2$ is the same as $\left(\frac{\gamma-1}{2}\right)\bar{u}_B - \bar{a}_B$, and $\left(\frac{\gamma-1}{2}\right)\bar{u}_2 + \bar{a}_2$ is found from Fig. 7a, from which $\bar{u}_2$ and $\bar{a}_2$ are computed. Figure 7d gives the value of $\bar{u}_1$ and $\bar{a}_1 = 1 - \left(\frac{\gamma-1}{2}\right)\bar{u}_1$. Along the upstream characteristic (1)-C in the chamber, $\bar{u} = \bar{u}_1$ and $\bar{a} = \bar{a}_1$. The launch tube characteristic can then be continued downstream from the chamber to the projectile path by previously discussed procedures. The upstream characteristic in the chamber is straight until intersection with the first reflected characteristic.

PATH OF THE FIRST REFLECTED CHARACTERISTIC IN CHAMBER

Throughout the chamber region, bounded by the first reflected characteristic, the following conditions obtain:

(1) The upstream characteristics are straight lines along which $\bar{u}$ and $\bar{a}$ are constant. The slope is $\bar{u}_1 - \bar{a}_1$.

(2) The downstream characteristics are given by $\left(\frac{\gamma-1}{2}\right)\bar{u} + \bar{a} = 1$.

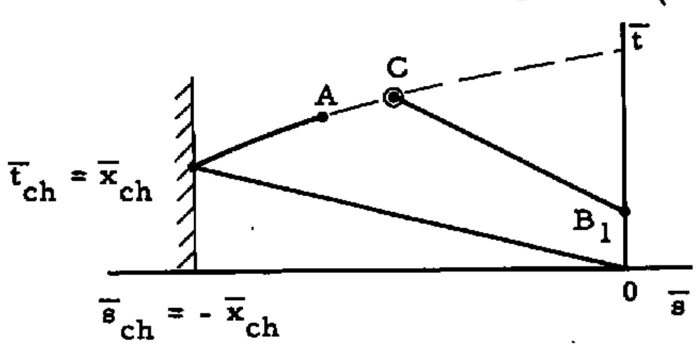

The slope of the first upstream characteristic is -1 since $\bar{u} = 0$ therefore

$$\bar{t}_{ch} = \bar{x}_{ch}$$

$$\bar{u} = 0$$

$$\bar{a}_{ch} = 1.0$$

The reflected characteristic can be completed as outlined for the general net intersection point with the following simplifications:

$$\left.\begin{aligned}\bar{a}_c &= \bar{a}_B \\ \bar{u}_c &= \bar{u}_B\end{aligned}\right\} \text{ at the chamber exit } B_1$$

$$\bar{a} = 1 - \left(\frac{\gamma - 1}{2}\right) \bar{u}$$

Computation Forms

Figure 8 shows computation forms that were found to be convenient in making the preceding calculations. Figure 8a was used for Interior Net Points, 8b for Projectile Path Points, and 8c for Chamber Exit Points. Using a desk calculator, 50 hours on the average was required to complete a solution.

RESULTS OF CHARACTERISTICS CALCULATIONS FOR FINITE CHAMBER VOLUME – γ = 1.66

Using the methods of the preceding sections, calculations were carried out for helium ($\gamma = 1.66$) as a propellant. The following table gives the geometrical variables considered:

Chambrage, A_1/A_2	Chamber Length, $\bar{X}_{ch}$
1	0.5, 1.0, 2.0, 4.0
4	0.125, 0.25, 0.5, ∞
∞	Any

The infinite chamber length case for $A_1/A_2 = 1$ is the closed form solution given in the first section (Fig. 2).

Figure 9 is a typical characteristics net; $A_1/A_2 = 4$ and $\bar{x}_{ch} = 0.5$. The coordinates are dimensionless time and distance:

$$\bar{t} = \frac{P_c A_L}{m_M a_c} t \qquad \text{and} \qquad \bar{s} = \frac{P_c A_L}{m_M a_c^2} s$$

where

P_c = Initial chamber pressure

a_c = Initial chamber acoustic speed

A_L = Launch tube area

m_M = Projectile mass

In Figs. 10 and 11, the dimensionless velocity and time are shown as functions of dimensionless distance for the cases calculated. $\bar{u}$ is defined as u_M/a_c. The reference solution for no chambrage and infinite chamber length is included because it provides a convenient basis for normalizing. It is interesting to observe that the compensating effects of chambrage and chamber length result in nearly the same velocity and time for equal chamber volumes.

In Fig. 12 the above observation is used to provide a convenient summary of the results of the characteristics calculations. Here the velocity is normalized to the reference case ($A_1/A_2 = 1$, $\bar{x}_{ch} \to \infty$) and plotted against volume of the chamber to volume of the launch tube for constant values of launch tube length, $\bar{s}$. It will be noted that larger chamber volumes are required for smaller $\bar{s}$. This is understandable when it is considered that small $\bar{s}$ is associated with large acoustic speed and therefore rapid communication of the decaying chamber pressure to the projectile base. The apparently anomalous results of certain experimental launchings with cold and hot propellants are thereby explained. For instance, in Ref. 6 very good correlation of launch velocity with chambrage was obtained using cold nitrogen as a propellant. In Ref. 5, however, Charters observes that in high temperature helium the velocity observed was best predicted by the no-chambrage reference formula. Similar results have been noted (Ref. 7) at AEDC for a H_2-O_2-He combustion-heated launcher, which has also been operated with cold helium. In these latter cases, the effects of chambrage and finite chamber volume approximately compensate in the hot firings ($\bar{s} = 4 - 10$), and in the cold launchings ($\bar{s} = 20 - 40$) the chambrage affects the velocity favorably.

A criterion for selecting the volume of a chamber for a given launch tube is considered in Ref. 2, which is the arrival of the first reflected characteristic at the end of the launch tube. This leads to excessively long chambers (Fig. 10) -- from one-fifth to one-half the launch tube length. It is suggested that a reasonable criterion might be derived from Fig. 12 as the chamber volume required to obtain the reference velocity, $\bar{u}_o$ ($A_1/A_2 = 1$, $\bar{x}_{ch} \to \infty$). In this case the chamber volume will be between 0.1 and 0.4 of the launch tube volume corresponding to $\bar{s}$ between 3 and 20, which is appropriate for light-gas launchers of high performance. Figure 13 shows this in simple form. It will be noted that a larger volume will be required with chambrage; however, the chamber will be shorter. Such a configuration is usually more convenient and, in addition, the surface-to-volume ratio is more favorable with respect to heat losses.

CONCLUSIONS

A characteristics method is outlined for an ideal propellant by which the performance of a model launcher can be computed. Both chambrage and finite chamber length are included. Dimensionless time-distance-velocity results are presented for chambrage area ratios of 1, 4, and ∞ and for several chamber lengths applicable to helium as a propellant.

The results are summarized to show the effect of finite chamber geometry on launch velocity. The volume of the chamber required for a given launch tube is presented. The influence of finite chamber volume is particularly important in the design of two-stage launchers where the volume after compression may be very small and therefore adversely affect performance.

ACKNOWLEDGMENT

The author wishes to acknowledge the valuable work of Mrs. C. Brantley in setting up the computation forms and in performing the calculations as well as preparing most of the figures.

REFERENCES

1. Courant, R. and Friedrichs, K. O. Supersonic Flow and Shock Waves. Interscience Publishers, Inc., New York, 1948.

2. Seigal, A. E. "The Influence of Chamber Diameter Size on the Muzzle Velocity of a Gun with Effectively an Infinite Length Chamber." NAVORD Report 3635, January 1954.

3. Heybey, W. "A Solution of La Grange's Problem of Interior Ballistics by Means of its Characteristic Lines." NOL Memorandum 10819, March 1950.

4. Cox, R. N. and Winter, D. F. T. "The Light-Gas Hypersonic Gun Tunnel at ARDE, Fort Halstead." AGARD Report No. 139, July 1957.

5. Charters, A. C., Denardo, P., and Rossow, V. J. "Development of a Piston-Compressor Type Light-Gas Gun for the Launching of Free-Flight Models at High Velocity." NACA-TN-4143, November 1957.

6. Seigal, A. E. and Dawson, V. C. D. "Results of Chambrage Experiments on Guns with Effectively Infinite Length Chambers." NOL Report 3636, April 1954.

7. Lord, M. E. "Performance of a 40-mm Combustion-Heated, Light-Gas Gun Launcher." AEDC-TN-60-176, October 1960.

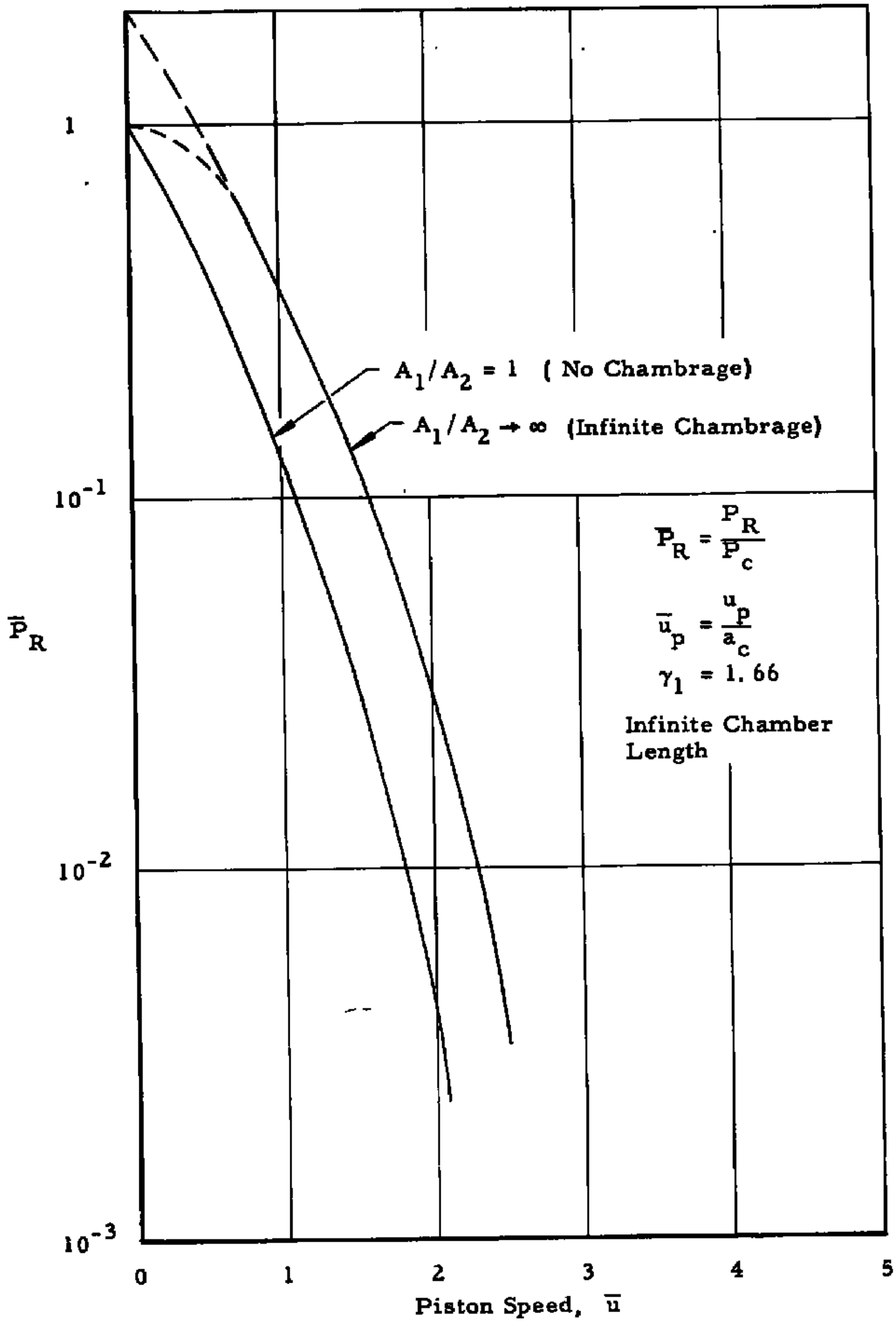

Fig. 1 Piston Rear Face Pressure as a Function of Speed

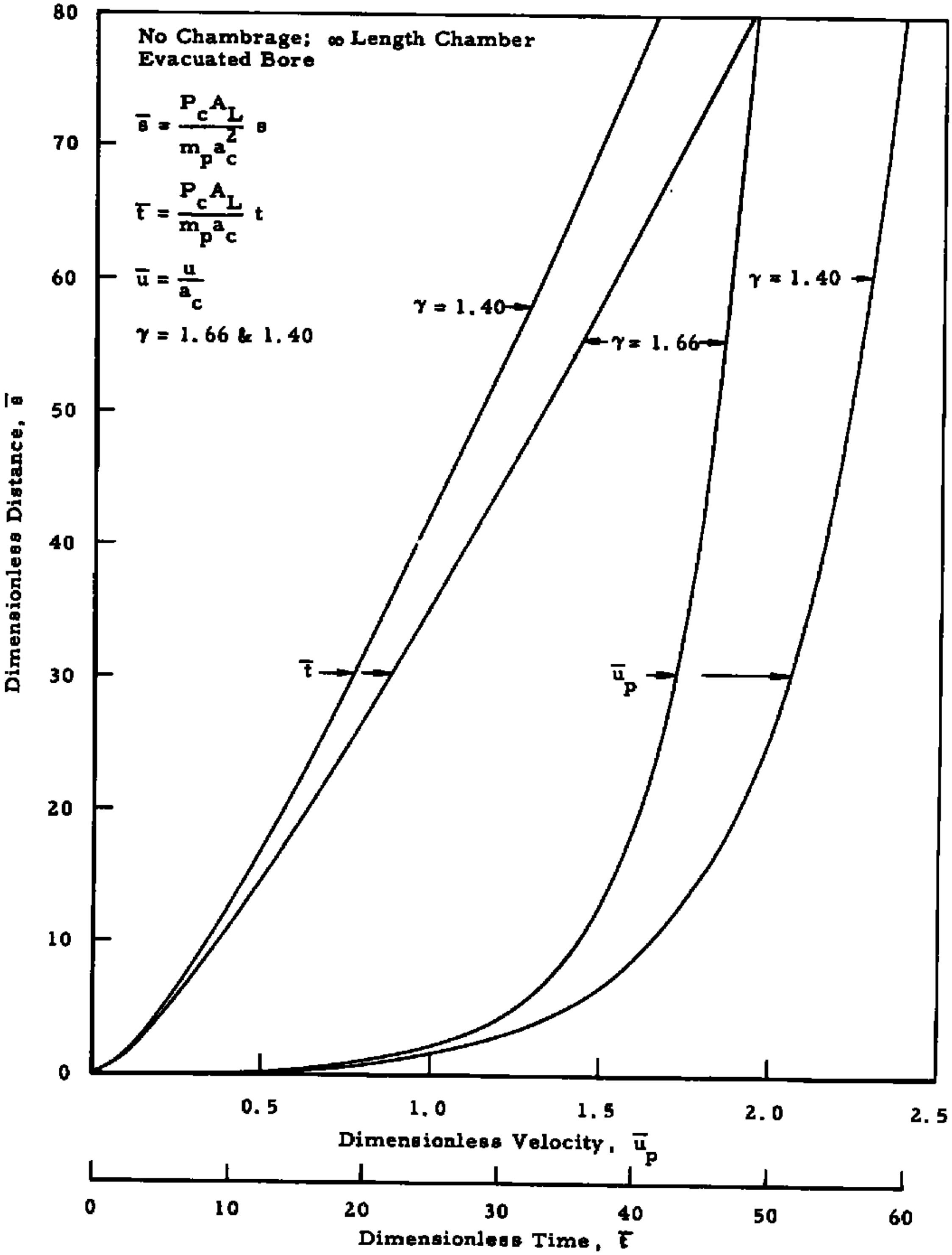

Fig. 2 Dimensionless Velocity and Time vs Dimensionless Projectile Travel

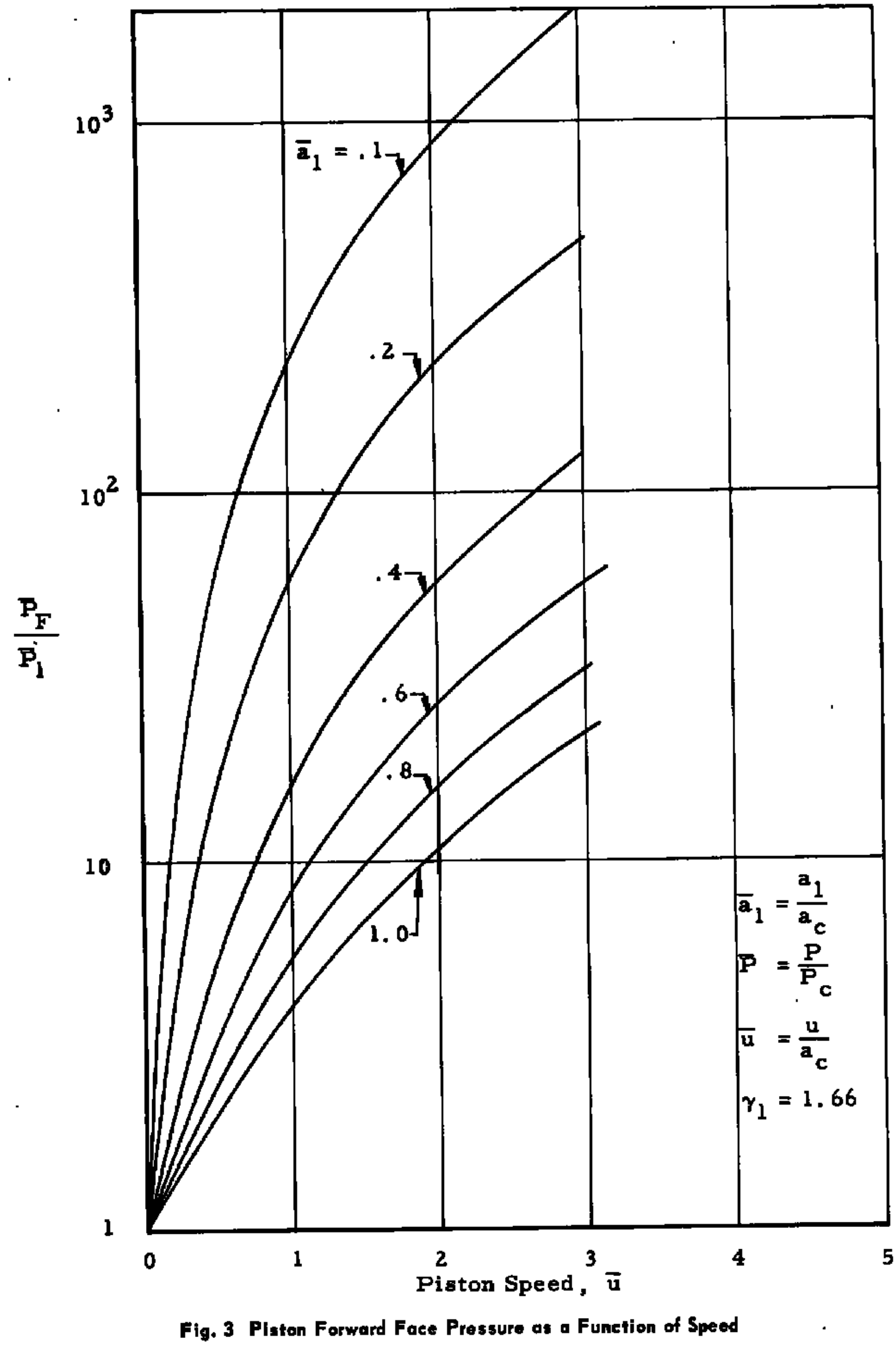

Fig. 3 Piston Forward Face Pressure as a Function of Speed

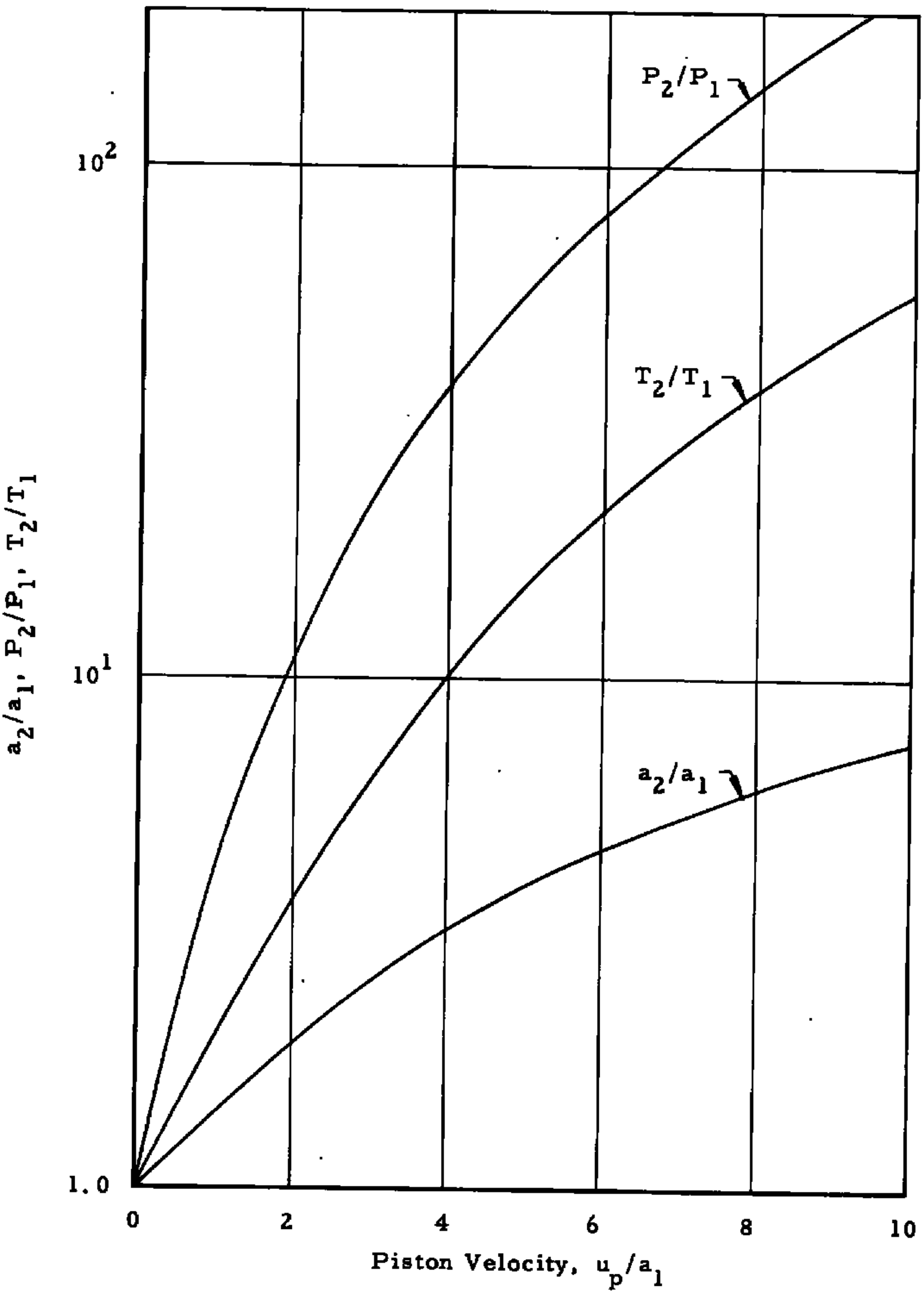

Fig. 4 Normal Shock in Helium

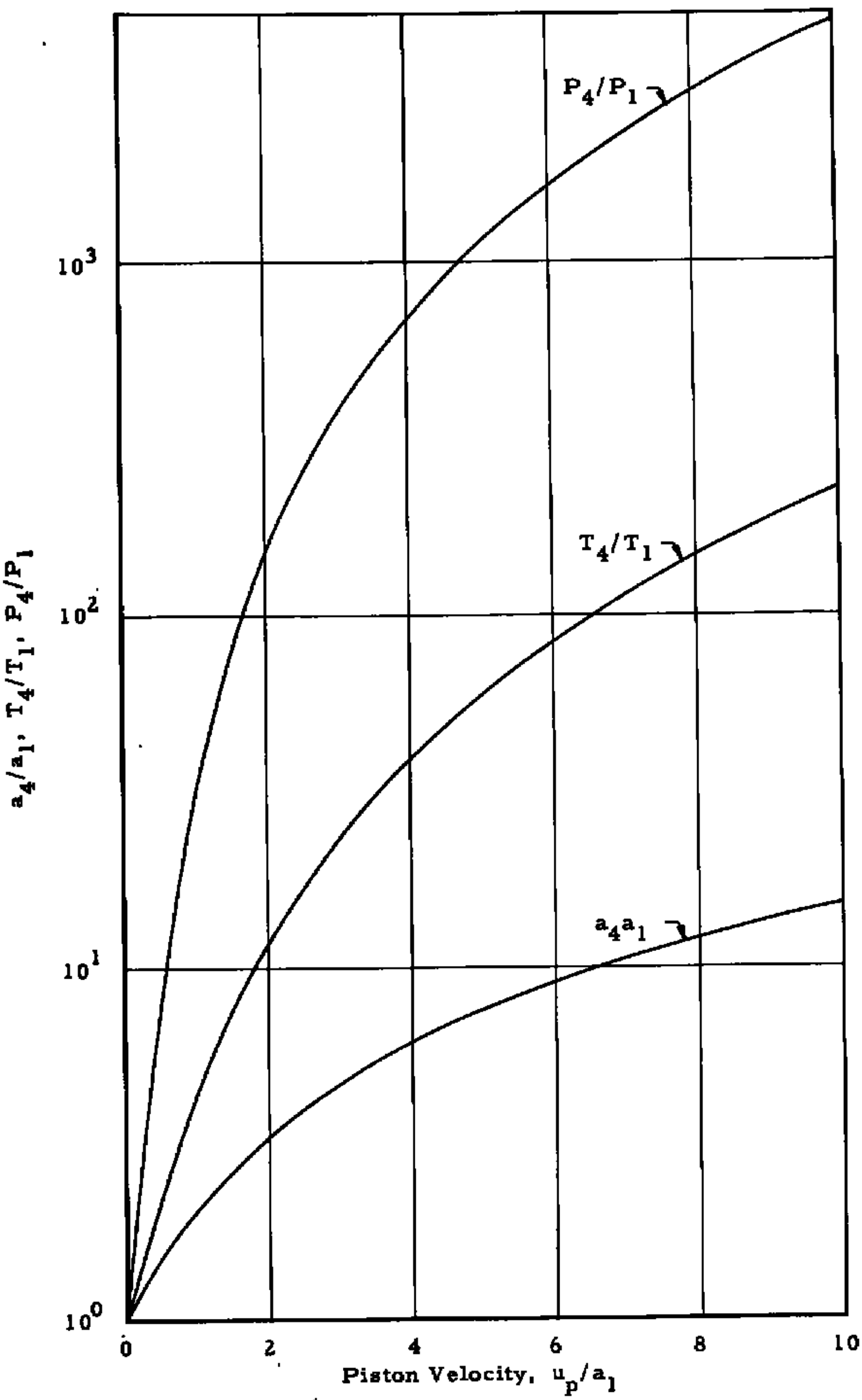

Fig. 5 Conditions after Three Shock Transits in Helium

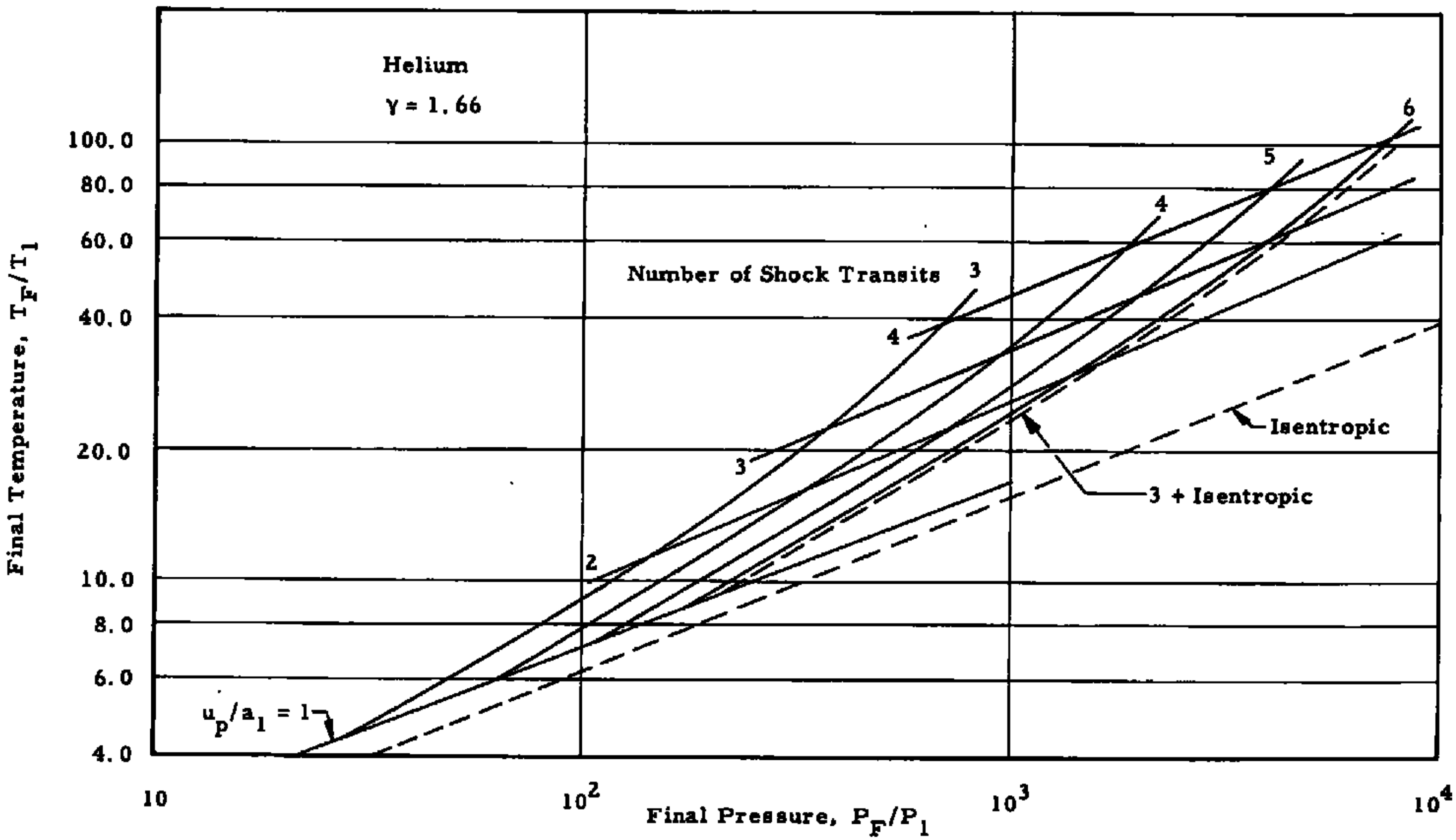

a. Temperature Ratio vs Pressure Ratio for Adiabatic Compressions

Fig. 6 Adiabatic Compression of Helium

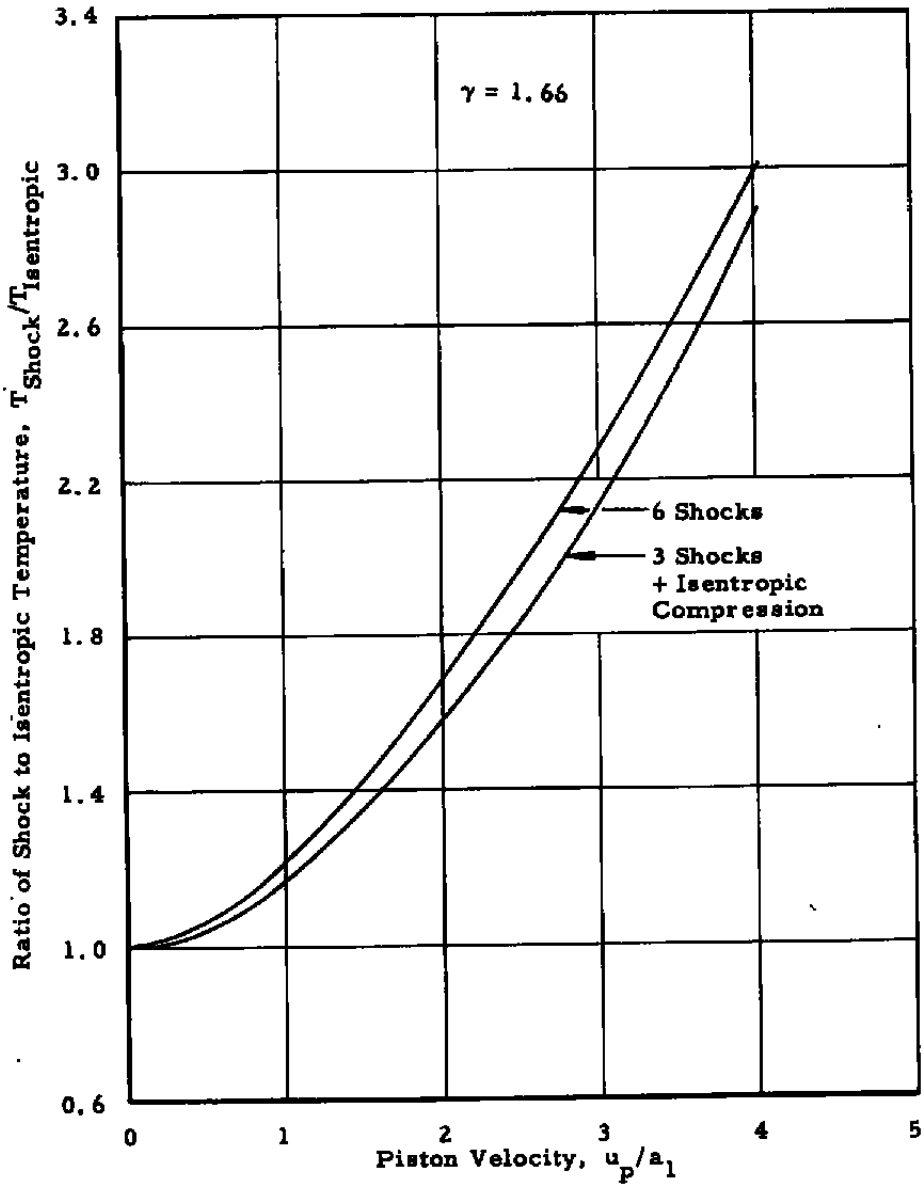

b. Ratio of Temperature in Shock Compression to Isentropic Compression as a Function of Piston Speed

Fig. 6 Concluded

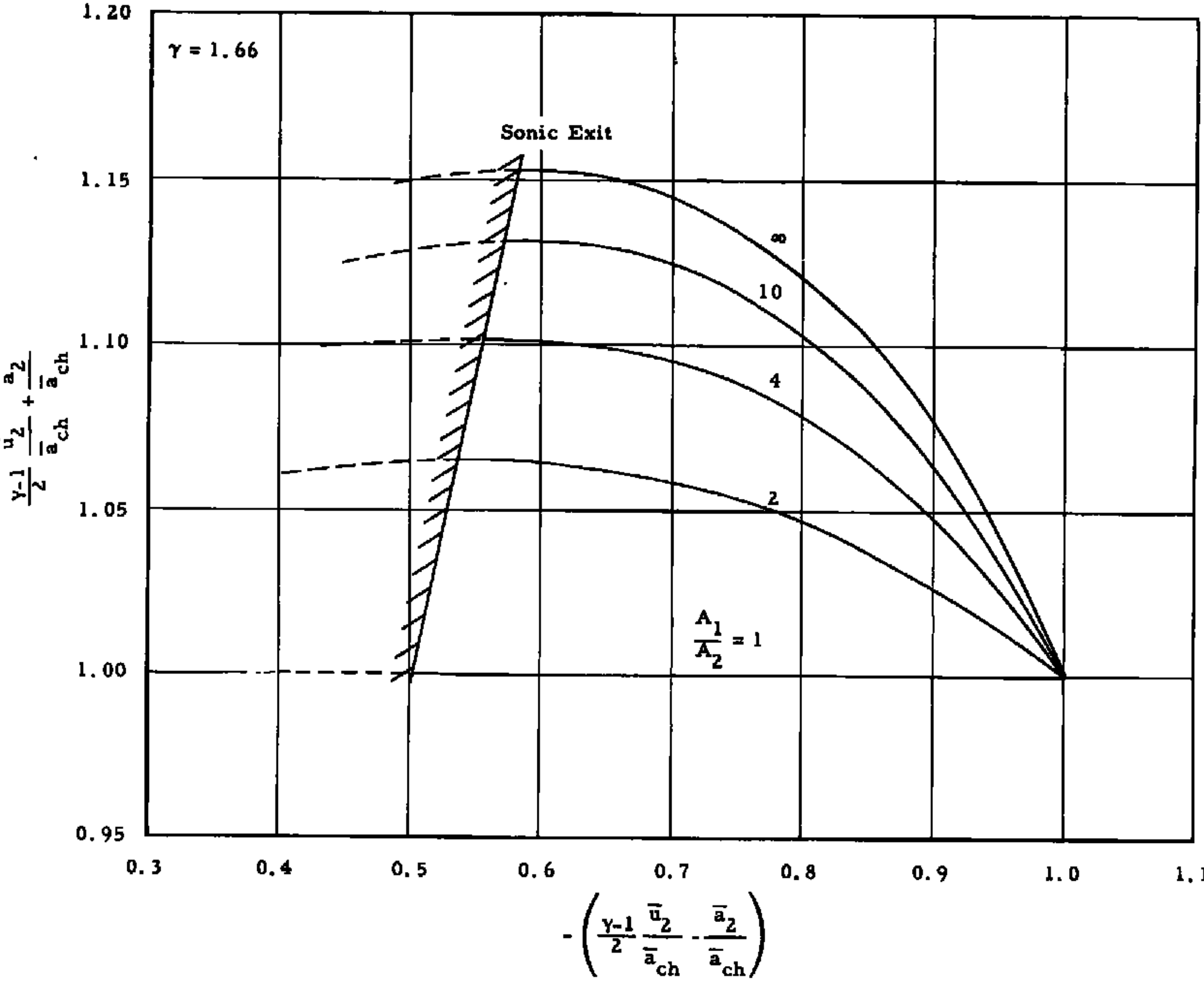

a. Downstream Characteristic Value at Chamber Exit

Fig. 7 Characteristic Relations across Chamber Exit

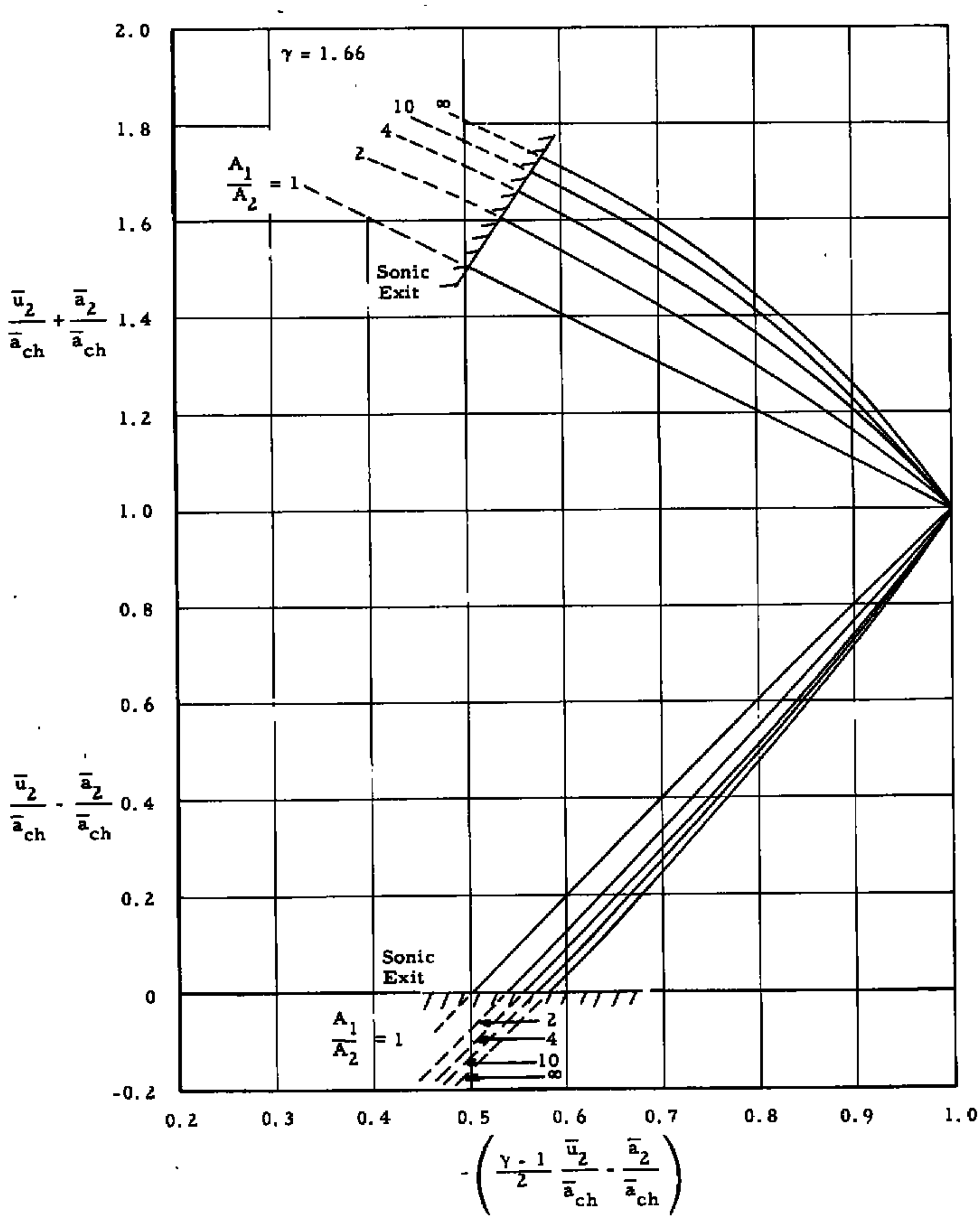

b. Characteristic Slopes at Chamber Exit

Fig. 7 Continued

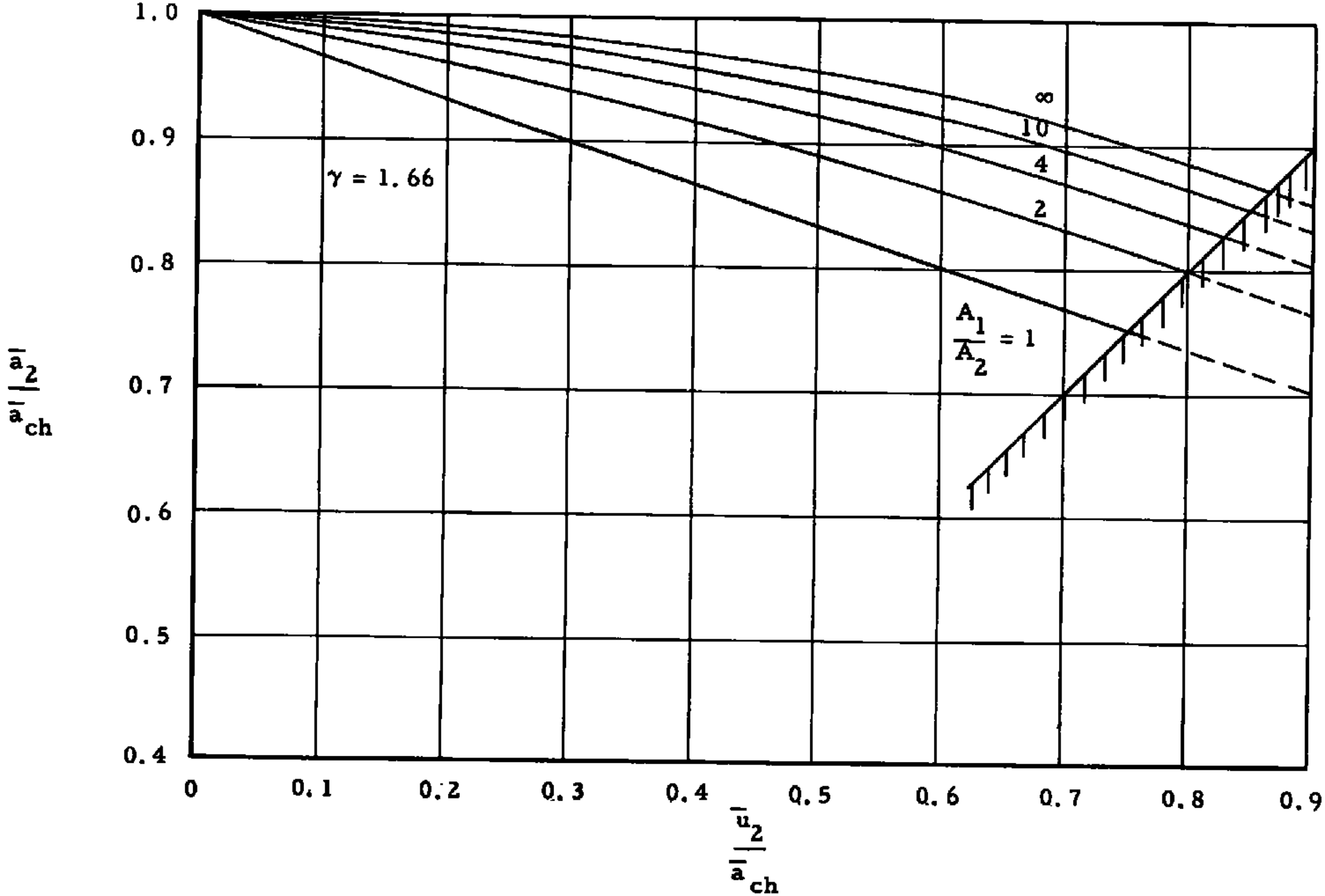

c. Chamber Exit Acoustic Speed vs Flow Speed

Fig. 7 Continued

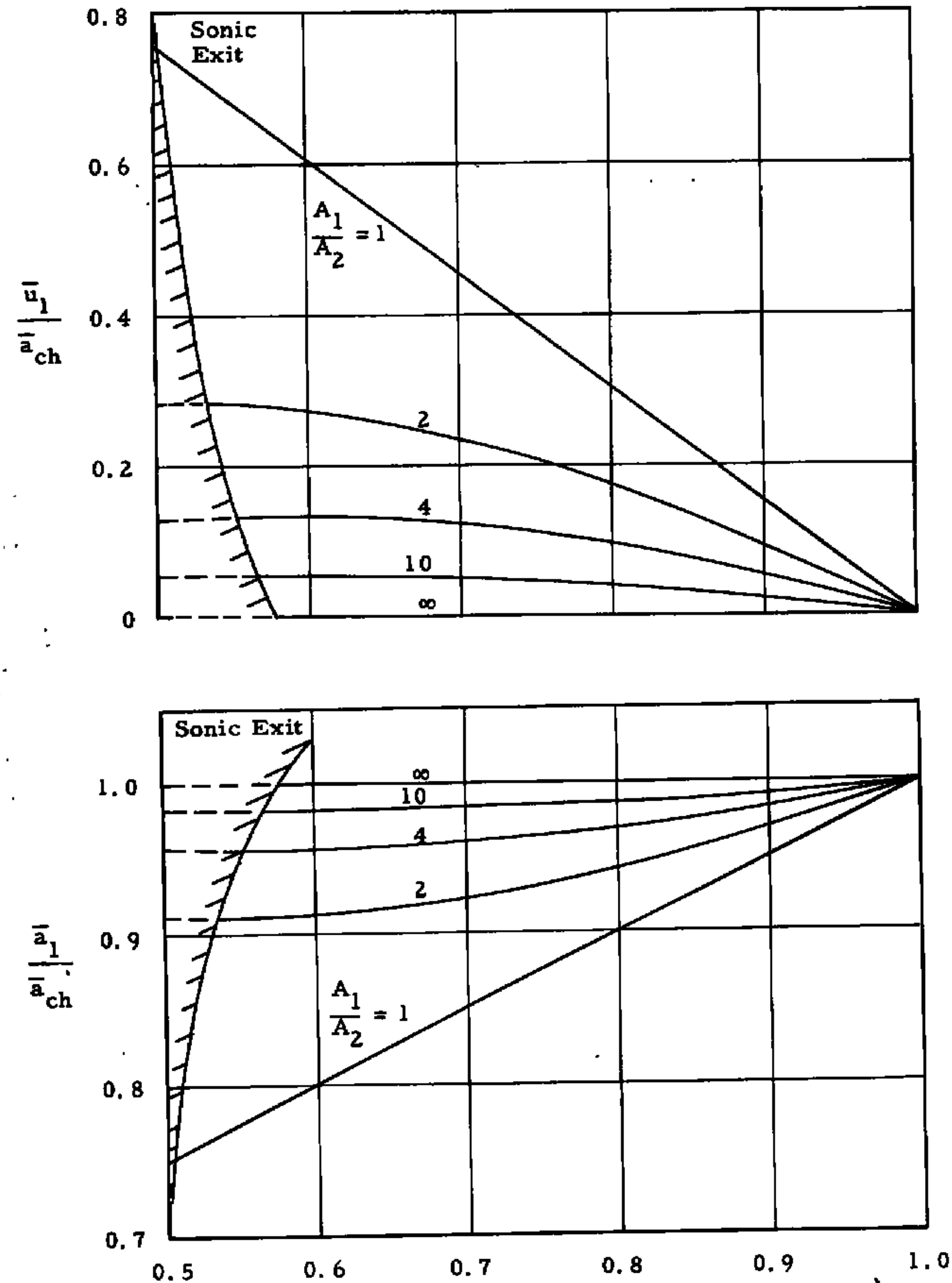

Upstream Characteristic Value , $-\left(\frac{\gamma - 1}{2}\frac{\bar{u}_2}{\bar{a}_{ch}} - \frac{\bar{a}_2}{\bar{a}_{ch}}\right)$

d. Entrance Velocities, $\bar{u}_1$ and $\bar{a}_1$

Fig. 7 Concluded

0	1	2	3	4	5	6	7	8	9	10	11	12	13	14	15	16	17	18	19
									$\frac{\gamma-1}{2}\bar{u}_A+\bar{a}_A$	$\frac{\gamma-1}{2}\bar{u}_B-\bar{a}_B$	$\bar{a}_C$	$\bar{u}_C$	α	β	$\alpha-\beta$	$2(\bar{S}_B-\bar{S}_A)$	$\bar{t}_C$	$\bar{t}_C-\bar{t}_A$	$\bar{S}_C$
Pt	$\bar{t}_A$	$\bar{S}_A$	$\bar{u}_A$	$\bar{a}_A$	$\bar{t}_B$	$\bar{S}_B$	$\bar{u}_B$	$\bar{a}_B$	.33(3)+(4)	.33(7)-(8)	$\frac{(9)-(10)}{2}$	$\frac{(9)-(11)}{.33}$	(3)+(4)+(11)+(12)	(7)-(8)+(12)-(11)	(13)-(14)	2 (6)-(2)	$\frac{(16)+(3)(13)-(5)(14)}{(15)}$	(17)-(1)	$\frac{(2)+(13)(18)}{2}$

a. Interior Net Points

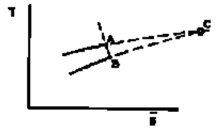

0	1	2	3	4	5	6	7	8	9	10	11	12	13	14	15	16	17	18	19	20
										α	β	$\alpha-\beta$	$\bar{S}_B-\bar{S}_A$	$\bar{t}_C$			$\bar{t}_C-\bar{t}_B$	$\bar{u}_C$	$\bar{a}_C$	$\bar{S}_C$
										except for $n=1$	except for $n=1$							See above for $n=1$		
Pt	n	$\bar{t}_A$	$\bar{S}_A$	$\bar{u}_A$	a_A	$\bar{t}_B$	$\bar{S}_B$	$\bar{u}_B$	$\bar{a}_B$	$\frac{(4)+(5)+\bar{u}_{C_{(n-1)}}+\bar{a}_{C_{(n-1)}}}{2}$	$\frac{(8)+\bar{u}_{C_{(n-1)}}}{2}$	(10)-(11)	(7)-(3)	$\frac{(13)+(10)(2)-(11)(6)}{12}$	$\bar{a}_B^{\frac{2\gamma}{\gamma-1}}$	$\bar{a}_{C_{(n-1)}}^{\frac{2\gamma}{\gamma-1}}$	(14)-(6)	$(8)+\left[\frac{(15)+(16)}{2}\times(17)\right]$	.33[(4)-(18)]+(5)	$(7)+\left[\frac{(8)+(18)}{2}\times(17)\right]$

b. Points on Projectile Path

0	1	2	3	4	5	6	7	8	9	10	11	12	13	14	15	16	17	18	19	20	21	22
						$\bar{t}$	$\frac{-(\frac{\gamma-1}{2}u_2-a_2)}{a_{ch}}$	$\frac{\gamma-1}{2}\bar{u}_2-\bar{a}_2$	$\frac{\gamma-1}{2}\bar{u}_2+\bar{a}_2$													
														Slope	Graphical							
$\bar{u}_1$	$\bar{a}_1$	$\bar{S}_A$	$\bar{u}_A$	$\bar{a}_A$	$\bar{t}_A$	$\frac{-2\bar{S}_A}{\bar{u}_A+\bar{a}_A+\bar{u}_1+\bar{a}_1}+\bar{t}_A$	From Plot	(7)×$\bar{a}_{ch}$	First Find $\frac{\frac{\gamma-1}{2}u_2+\bar{a}_2}{\bar{a}_{ch}}\times\bar{a}_{ch}$	$\bar{u}_2$	$\bar{a}_2$	$\bar{u}$	$\bar{a}$	$\frac{\bar{u}_2-\bar{a}_2+\bar{u}-\bar{a}}{2}$	$\frac{\gamma-1}{2}\bar{u}_2-\bar{a}_2$	$\frac{\frac{\gamma-1}{2}\bar{u}_2-\bar{a}_2}{\bar{a}_{ch}}$	$\frac{\bar{u}_1}{\bar{a}_{ch}}$	$\bar{u}_1$	$\bar{a}_1$	$\bar{t}_1$	$\bar{u}_2$	$\bar{a}_2$

c. Points at Chamber Exit

Fig. 8 Computation Forms

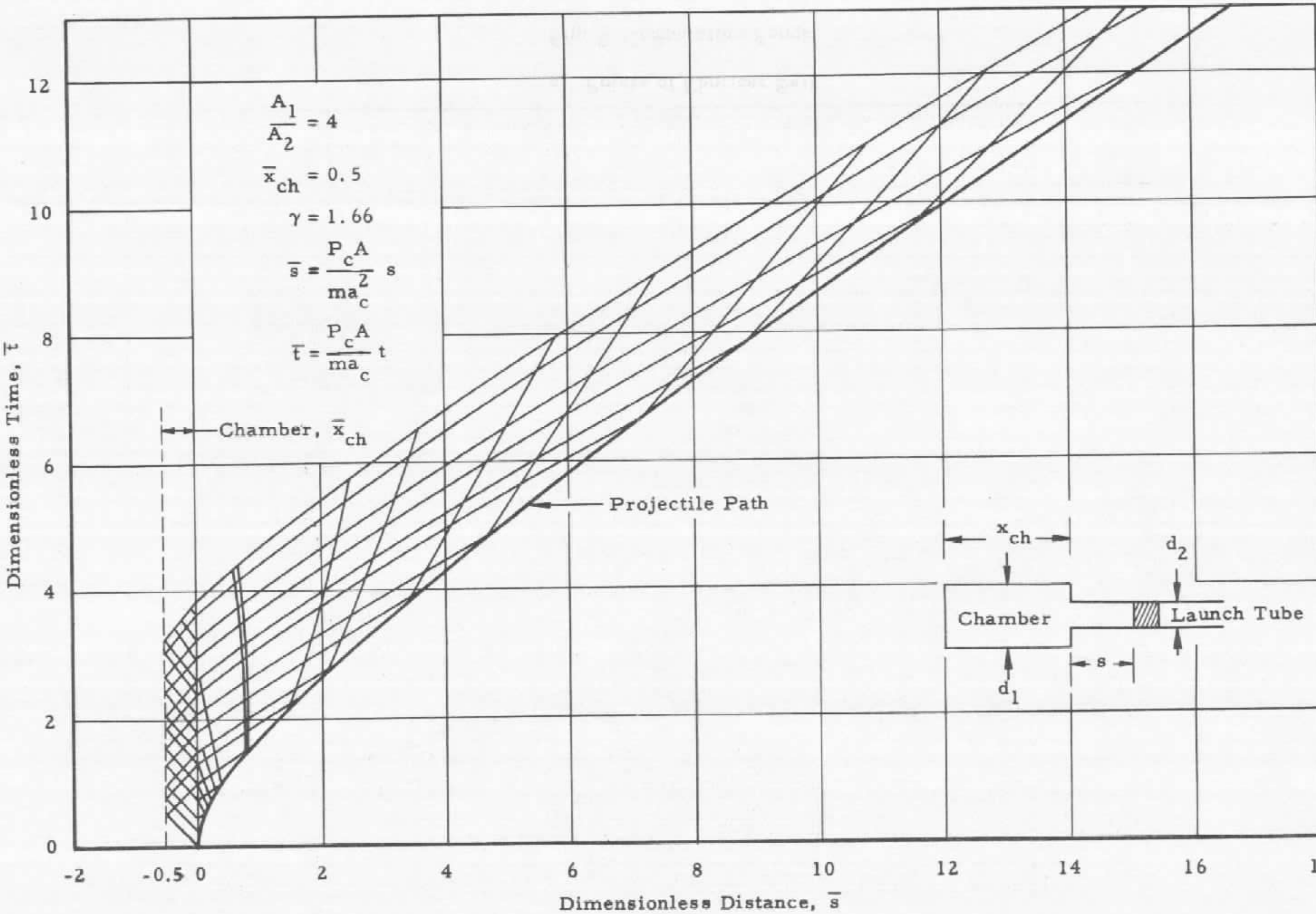

Fig. 9 Typical Characteristics Net for Finite Chamber Volume

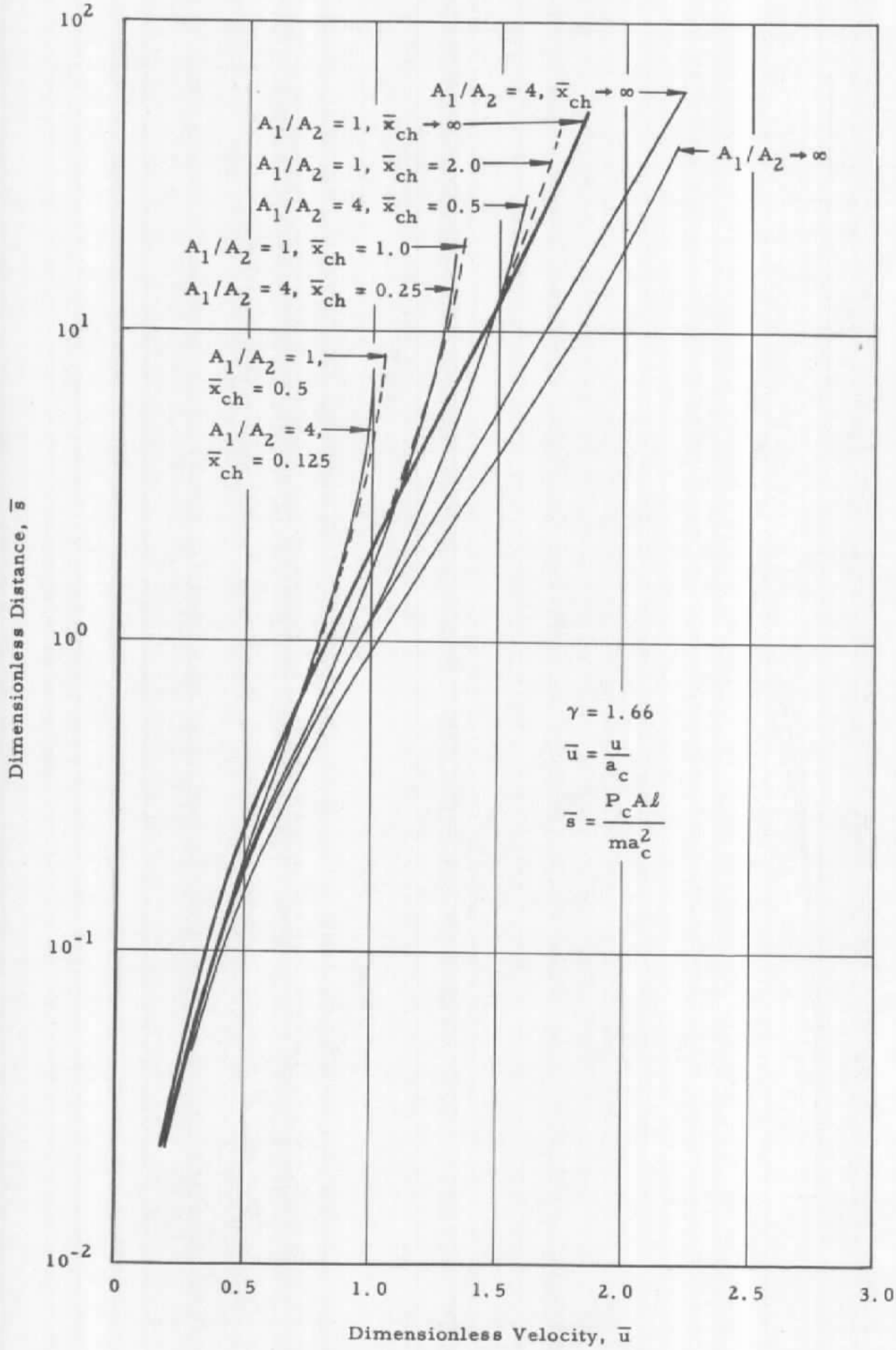

Fig. 10 Effect of Chamber Geometry on Velocity

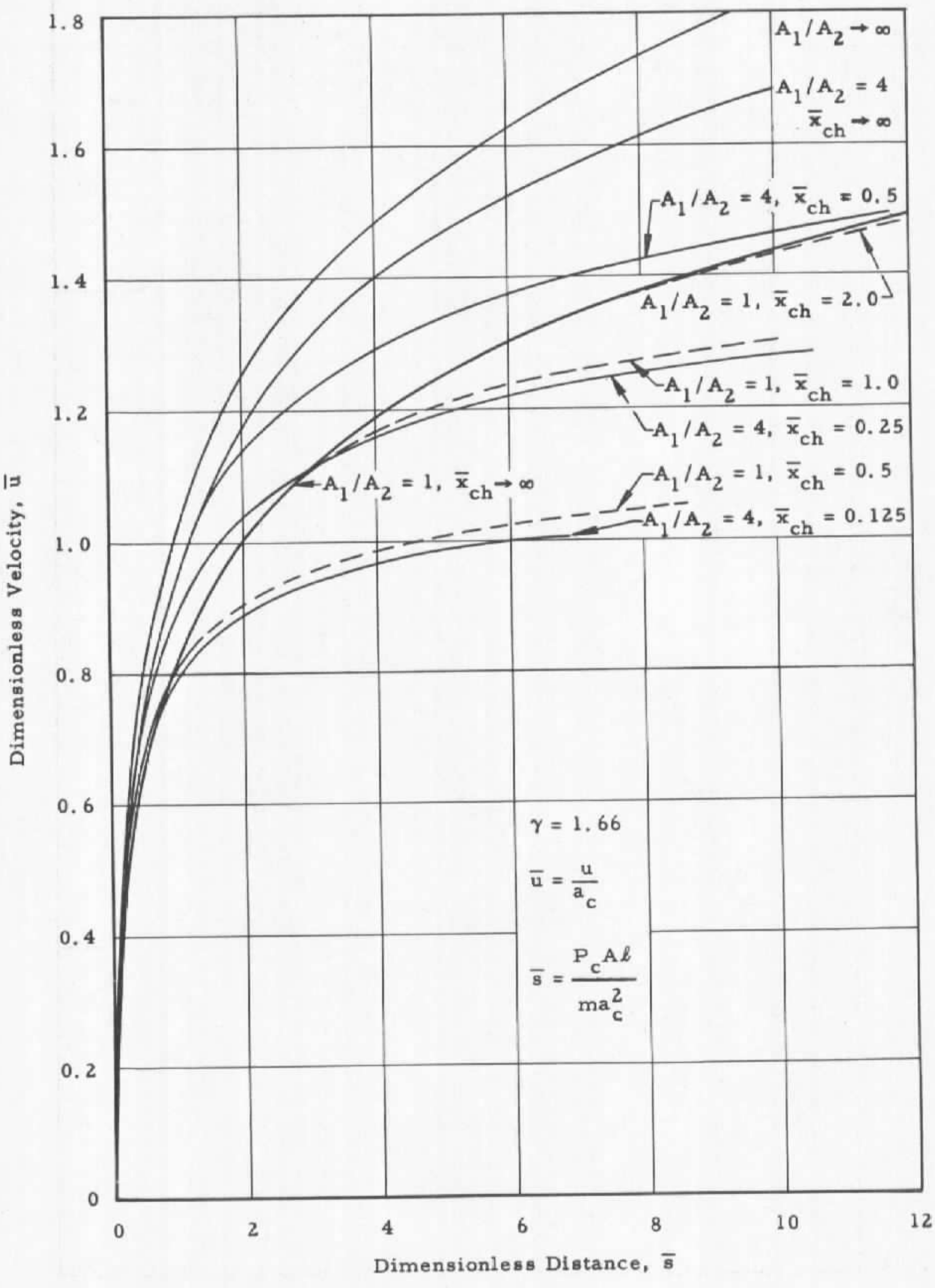

Fig. 10 Concluded

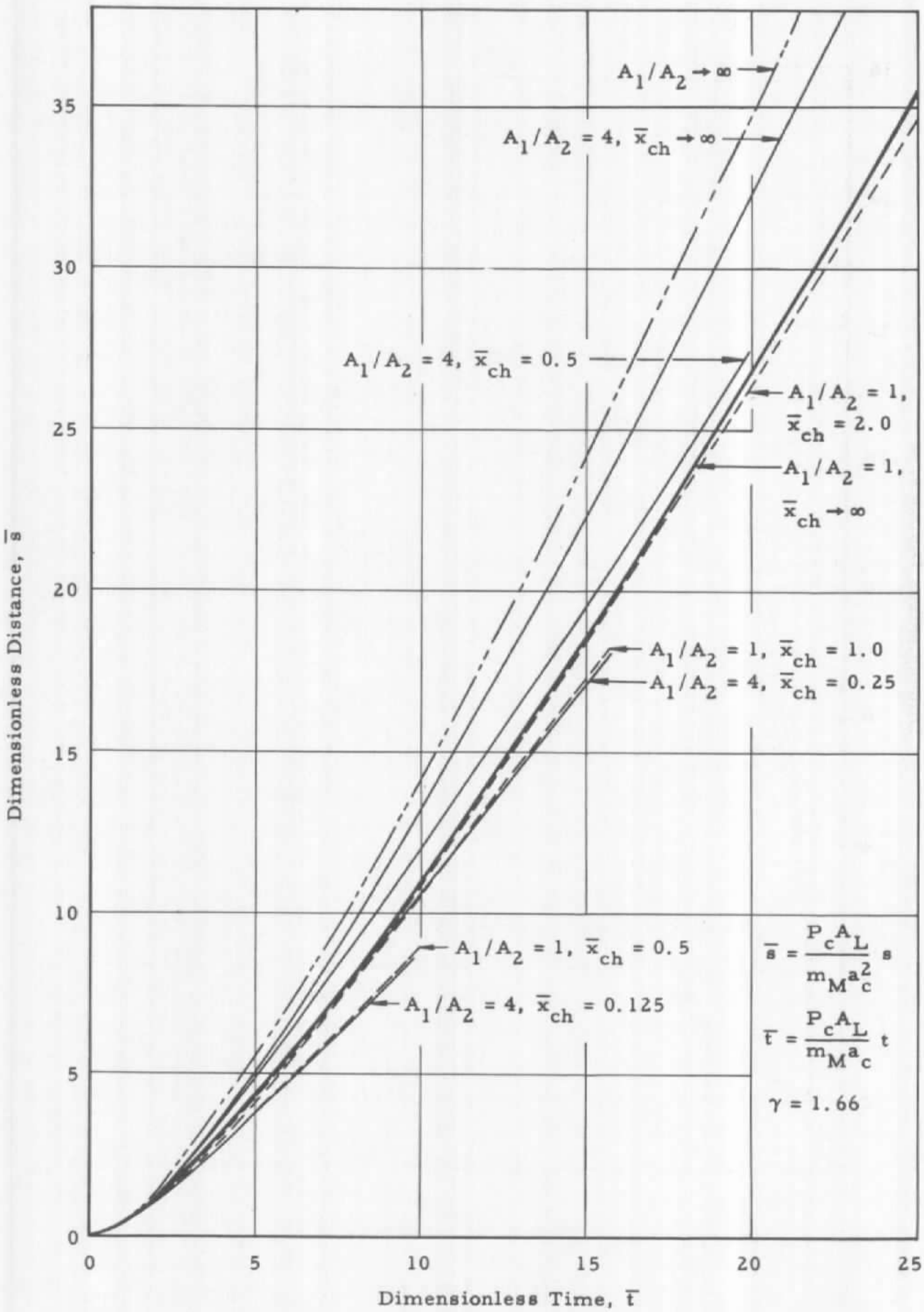

Fig. 11 Effect of Chamber Geometry on Dimensionless Time – Distance Relationship

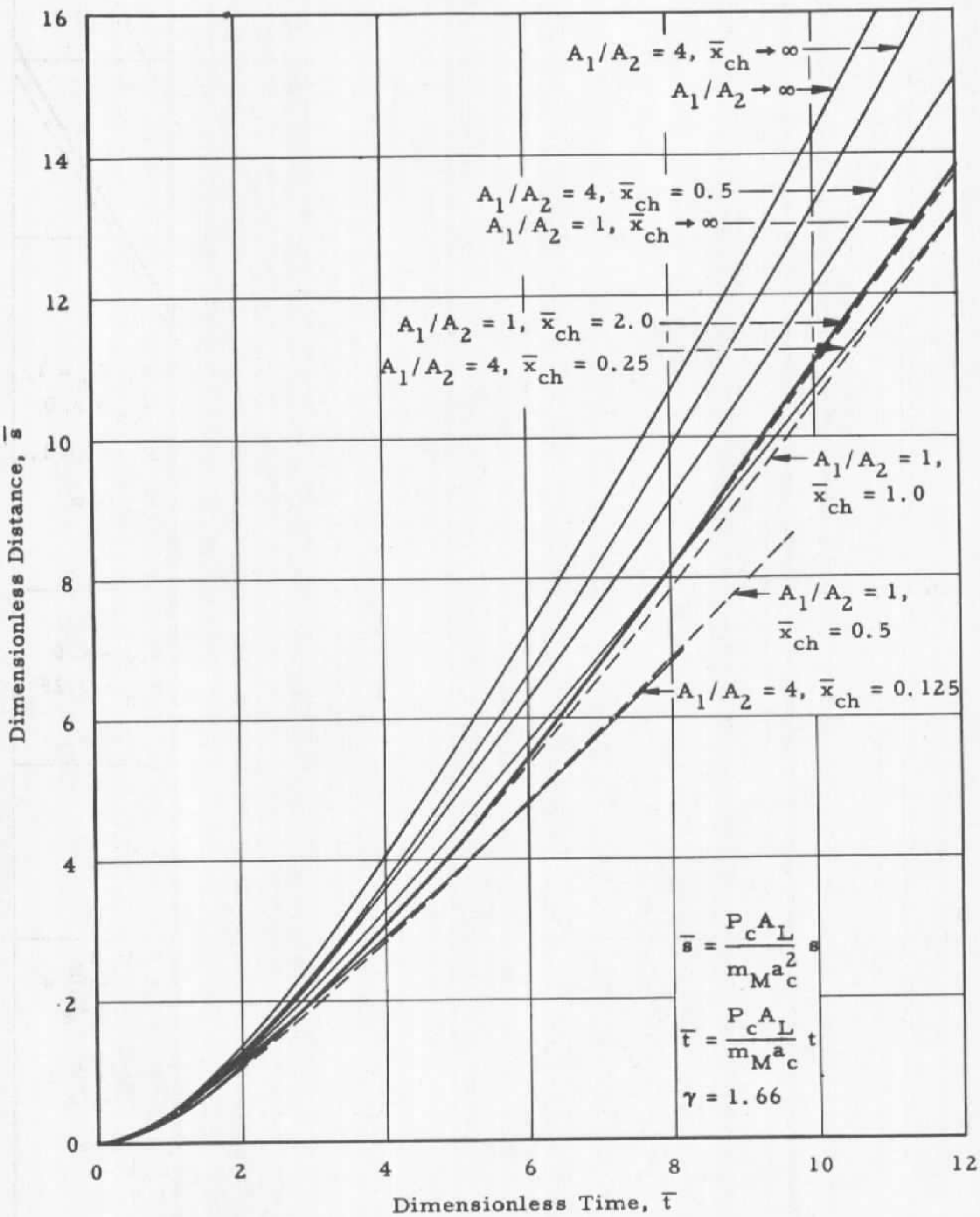

Fig. 11 Concluded

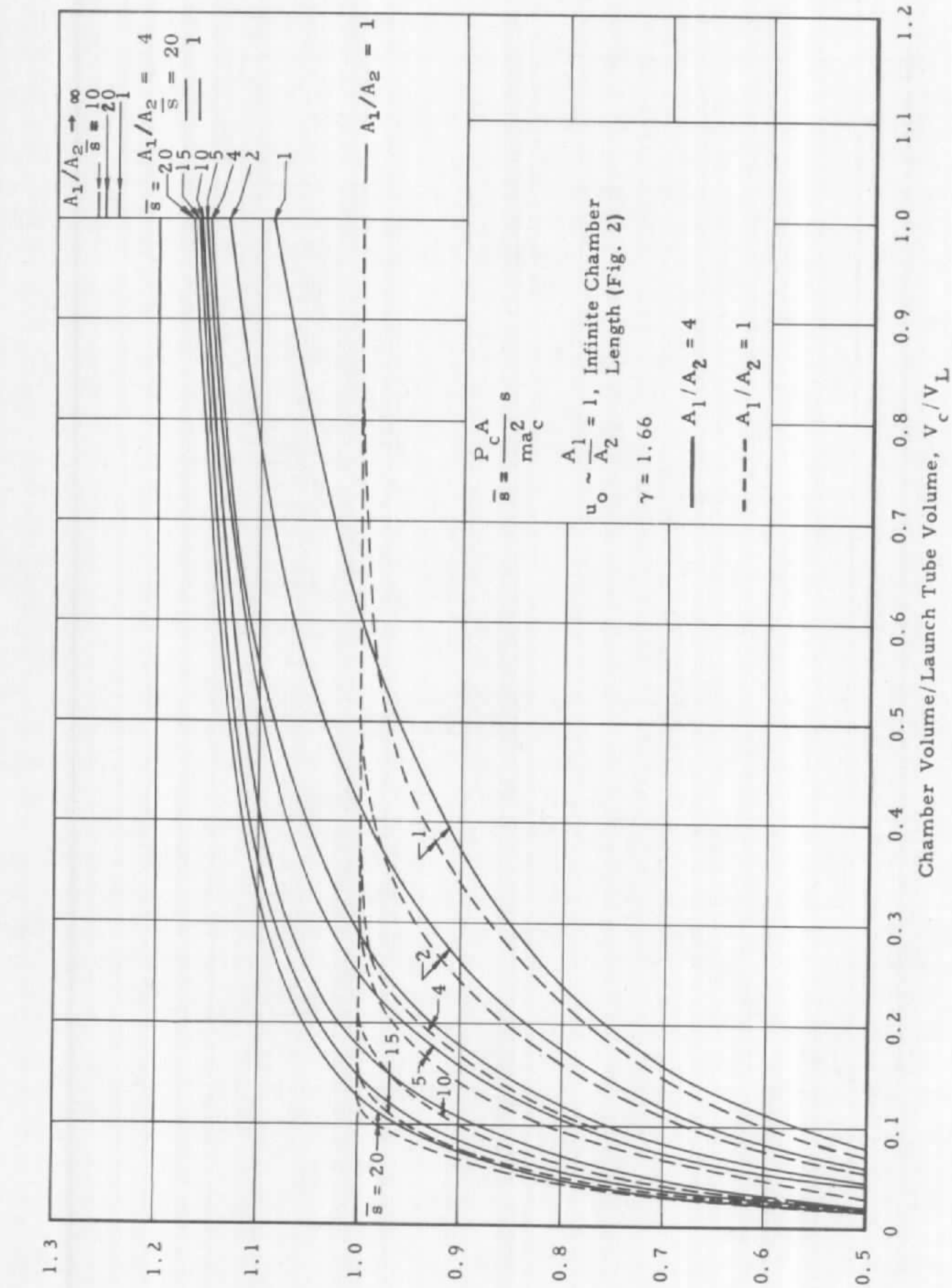

Fig. 12 Effect of Chamber/Launch Tube Volume Ratio on Launch Velocity

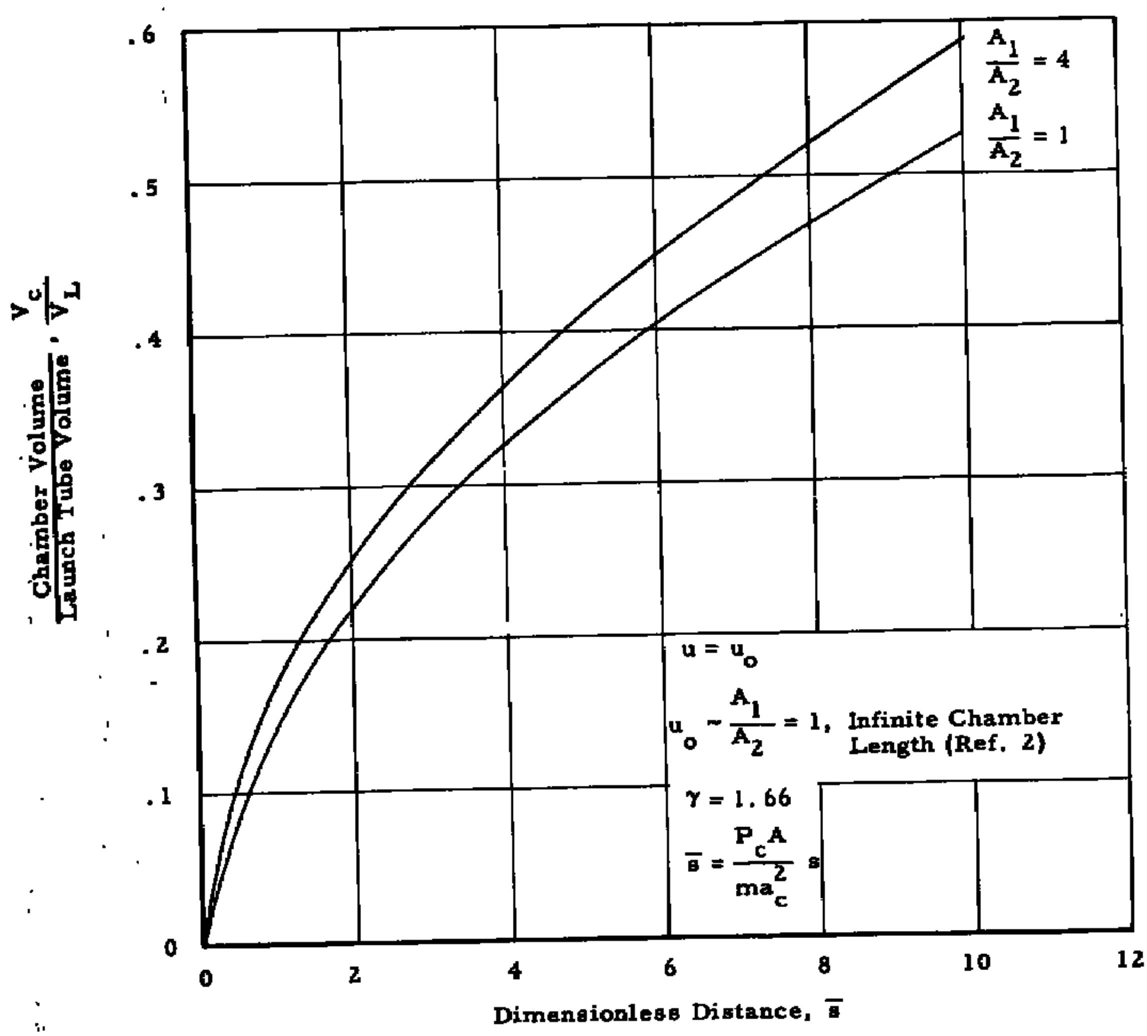

Fig. 13 Chamber Volume Required to Produce Ideal Launch Velocity

Cut on broken line

AEDC-TR-61-1

UNCLASSIFIED

Arnold Engineering Development Center, ARO, Inc., Arnold Air Force Station, Tennessee
THEORETICAL LIGHT-GAS GUN PERFORMANCE by W. B. Stephenson, May 1961. 49 pp. (ARO Project No. 386079) (AFSC Program Area 750A, Project No. 8950, Task 89600) (AEDC-TR-61-1) (Contract No. AF 40(600)-800 S/A 11(60-110)). Unclassified

7 references

One-dimensional, unsteady flow theory of an ideal gas is reviewed as it applies to guns and ballistic model launchers. The method of characteristics is developed for the general case including chambrage and finite chamber volume. Results for helium as a propellant are given from which the required chamber size can be determined. The launch velocity for combinations of launch tube and chamber geometries is computed assuming no friction nor heat loss and an evacuated bore.

1. Hypervelocity guns
2. Aeroballistics
3. Light-gas guns--Performance--Theory
4. Gas flow--Theory
5. Helium

I. Stephenson, W. B.

UNCLASSIFIED

AEDC-TR-61-1

UNCLASSIFIED

Arnold Engineering Development Center, ARO, Inc., Arnold Air Force Station, Tennessee
THEORETICAL LIGHT-GAS GUN PERFORMANCE by W. B. Stephenson, May 1961. 49 pp. (ARO Project No. 386079) (AFSC Program Area 750A, Project No. 8950, Task 89600) (AEDC-TR-61-1) (Contract No. AF 40(600)-800 S/A 11(60-110)). Unclassified

7 references

One-dimensional, unsteady flow theory of an ideal gas is reviewed as it applies to guns and ballistic model launchers. The method of characteristics is developed for the general case including chambrage and finite chamber volume. Results for helium as a propellant are given from which the required chamber size can be determined. The launch velocity for combinations of launch tube and chamber geometries is computed assuming no friction nor heat loss and an evacuated bore.

1. Hypervelocity guns
2. Aeroballistics
3. Light-gas guns--Performance--Theory
4. Gas flow--Theory
5. Helium

I. Stephenson, W. B.

UNCLASSIFIED

AEDC-TR-61-1

UNCLASSIFIED

Arnold Engineering Development Center, ARO, Inc., Arnold Air Force Station, Tennessee
THEORETICAL LIGHT-GAS GUN PERFORMANCE by W. B. Stephenson, May 1961. 49 pp. (ARO Project No. 386079) (AFSC Program Area 750A, Project No. 8950, Task 89600) (AEDC-TR-61-1) (Contract No. AF 40(600)-800 S/A 11(60-110)). Unclassified

7 references

One-dimensional, unsteady flow theory of an ideal gas is reviewed as it applies to guns and ballistic model launchers. The method of characteristics is developed for the general case including chambrage and finite chamber volume. Results for helium as a propellant are given from which the required chamber size can be determined. The launch velocity for combinations of launch tube and chamber geometries is computed assuming no friction nor heat loss and an evacuated bore.

1. Hypervelocity guns
2. Aeroballistics
3. Light-gas guns--Performance--Theory
4. Gas flow--Theory
5. Helium

I. Stephenson, W. B.

UNCLASSIFIED

AEDC-TR-61-1

UNCLASSIFIED

Arnold Engineering Development Center, ARO, Inc., Arnold Air Force Station, Tennessee
THEORETICAL LIGHT-GAS GUN PERFORMANCE by W. B. Stephenson, May 1961. 49 pp. (ARO Project No. 386079) (AFSC Program Area 750A, Project No. 8950, Task 89600) (AEDC-TR-61-1) (Contract No. AF 40(600)-800 S/A 11(60-110)). Unclassified

7 references

One-dimensional, unsteady flow theory of an ideal gas is reviewed as it applies to guns and ballistic model launchers. The method of characteristics is developed for the general case including chambrage and finite chamber volume. Results for helium as a propellant are given from which the required chamber size can be determined. The launch velocity for combinations of launch tube and chamber geometries is computed assuming no friction nor heat loss and an evacuated bore.

1. Hypervelocity guns
2. Aeroballistics
3. Light-gas guns--Performance--Theory
4. Gas flow--Theory
5. Helium

I. Stephenson, W. B.

UNCLASSIFIED

Cut on broken line

AEDC-TR-61-1

Arnold Engineering Development Center, ARO, Inc., Arnold Air Force Station, Tennessee
THEORETICAL LIGHT-GAS GUN PERFORMANCE by W. B. Stephenson, May 1961. 49 pp. (ARO Project No. 386079) (AFSC Program Area 750A, Project No. 8950, Task 89600) (AEDC-TR-61-1) (Contract No. AF 40(600)-800 S/A 11(60-110)). Unclassified

7 references

One-dimensional, unsteady flow theory of an ideal gas is reviewed as it applies to guns and ballistic model launchers. The method of characteristics is developed for the general case including chambrage and finite chamber volume. Results for helium as a propellant are given from which the required chamber size can be determined. The launch velocity for combinations of launch tube and chamber geometries is computed assuming no friction nor heat loss and an evacuated bore.

UNCLASSIFIED

1. Hypervelocity guns
2. Aeroballistics
3. Light-gas guns--Performance--Theory
4. Gas flow--Theory
5. Helium
I. Stephenson, W. B.

UNCLASSIFIED

AEDC-TR-61-1

Arnold Engineering Development Center, ARO, Inc., Arnold Air Force Station, Tennessee
THEORETICAL LIGHT-GAS GUN PERFORMANCE by W. B. Stephenson, May 1961. 49 pp. (ARO Project No. 386079) (AFSC Program Area 750A, Project No. 8950, Task 89600) (AEDC-TR-61-1) (Contract No. AF 40(600)-800 S/A 11(60-110)). Unclassified

7 references

One-dimensional, unsteady flow theory of an ideal gas is reviewed as it applies to guns and ballistic model launchers. The method of characteristics is developed for the general case including chambrage and finite chamber volume. Results for helium as a propellant are given from which the required chamber size can be determined. The launch velocity for combinations of launch tube and chamber geometries is computed assuming no friction nor heat loss and an evacuated bore.

UNCLASSIFIED

1. Hypervelocity guns
2. Aeroballistics
3. Light-gas guns--Performance--Theory
4. Gas flow--Theory
5. Helium
I. Stephenson, W. B.

UNCLASSIFIED

AEDC-TR-61-1

Arnold Engineering Development Center, ARO, Inc., Arnold Air Force Station, Tennessee
THEORETICAL LIGHT-GAS GUN PERFORMANCE by W. B. Stephenson, May 1961. 49 pp. (ARO Project No. 386079) (AFSC Program Area 750A, Project No. 8950, Task 89600) (AEDC-TR-61-1) (Contract No. AF 40(600)-800 S/A 11(60-110)). Unclassified

7 references

One-dimensional, unsteady flow theory of an ideal gas is reviewed as it applies to guns and ballistic model launchers. The method of characteristics is developed for the general case including chambrage and finite chamber volume. Results for helium as a propellant are given from which the required chamber size can be determined. The launch velocity for combinations of launch tube and chamber geometries is computed assuming no friction nor heat loss and an evacuated bore.

UNCLASSIFIED

1. Hypervelocity guns
2. Aeroballistics
3. Light-gas guns--Performance--Theory
4. Gas flow--Theory
5. Helium
I. Stephenson, W. B.

UNCLASSIFIED

AEDC-TR-61-1

Arnold Engineering Development Center, ARO, Inc., Arnold Air Force Station, Tennessee
THEORETICAL LIGHT-GAS GUN PERFORMANCE by W. B. Stephenson, May 1961. 49 pp. (ARO Project No. 386079) (AFSC Program Area 750A, Project No. 8950, Task 89600) (AEDC-TR-61-1) (Contract No. AF 40(600)-800 S/A 11(60-110)). Unclassified

7 references

One-dimensional, unsteady flow theory of an ideal gas is reviewed as it applies to guns and ballistic model launchers. The method of characteristics is developed for the general case including chambrage and finite chamber volume. Results for helium as a propellant are given from which the required chamber size can be determined. The launch velocity for combinations of launch tube and chamber geometries is computed assuming no friction nor heat loss and an evacuated bore.

UNCLASSIFIED

1. Hypervelocity guns
2. Aeroballistics
3. Light-gas guns--Performance--Theory
4. Gas flow--Theory
5. Helium
I. Stephenson, W. B.

UNCLASSIFIED

Cut on broken line

AEDC-TR-61-1

UNCLASSIFIED

Arnold Engineering Development Center, ARO, Inc., Arnold Air Force Station, Tennessee
THEORETICAL LIGHT-GAS GUN PERFORMANCE by W. B. Stephenson, May 1961. 49 pp. (ARO Project No. 386079) (AFSC Program Area 750A, Project No. 8950, Task 89600) (AEDC-TR-61-1) (Contract No. AF 40(600)-800 S/A 11(60-110)). Unclassified

7 references

One-dimensional, unsteady flow theory of an ideal gas is reviewed as it applies to guns and ballistic model launchers. The method of characteristics is developed for the general case including chambrage and finite chamber volume. Results for helium as a propellant are given from which the required chamber size can be determined. The launch velocity for combinations of launch tube and chamber geometries is computed assuming no friction nor heat loss and an evacuated bore.

1. Hypervelocity guns
2. Aeroballistics
3. Light-gas guns--Performance--Theory
4. Gas flow--Theory
5. Helium
I. Stephenson, W. B.

UNCLASSIFIED

AEDC-TR-61-1

UNCLASSIFIED

Arnold Engineering Development Center, ARO, Inc., Arnold Air Force Station, Tennessee
THEORETICAL LIGHT-GAS GUN PERFORMANCE by W. B. Stephenson, May 1961. 49 pp. (ARO Project No. 386079) (AFSC Program Area 750A, Project No. 8950, Task 89600) (AEDC-TR-61-1) (Contract No. AF 40(600)-800 S/A 11(60-110)). Unclassified

7 references

One-dimensional, unsteady flow theory of an ideal gas is reviewed as it applies to guns and ballistic model launchers. The method of characteristics is developed for the general case including chambrage and finite chamber volume. Results for helium as a propellant are given from which the required chamber size can be determined. The launch velocity for combinations of launch tube and chamber geometries is computed assuming no friction nor heat loss and an evacuated bore.

1. Hypervelocity guns
2. Aeroballistics
3. Light-gas guns--Performance--Theory
4. Gas flow--Theory
5. Helium
I. Stephenson, W. B.

UNCLASSIFIED

AEDC-TR-61-1

UNCLASSIFIED

Arnold Engineering Development Center, ARO, Inc., Arnold Air Force Station, Tennessee
THEORETICAL LIGHT-GAS GUN PERFORMANCE by W. B. Stephenson, May 1961. 49 pp. (ARO Project No. 386079) (AFSC Program Area 750A, Project No. 8950, Task 89600) (AEDC-TR-61-1) (Contract No. AF 40(600)-800 S/A 11(60-110)). Unclassified

7 references

One-dimensional, unsteady flow theory of an ideal gas is reviewed as it applies to guns and ballistic model launchers. The method of characteristics is developed for the general case including chambrage and finite chamber volume. Results for helium as a propellant are given from which the required chamber size can be determined. The launch velocity for combinations of launch tube and chamber geometries is computed assuming no friction nor heat loss and an evacuated bore.

1. Hypervelocity guns
2. Aeroballistics
3. Light-gas guns--Performance--Theory
4. Gas flow--Theory
5. Helium
I. Stephenson, W. B.

UNCLASSIFIED

AEDC-TR-61-1

UNCLASSIFIED

Arnold Engineering Development Center, ARO, Inc., Arnold Air Force Station, Tennessee
THEORETICAL LIGHT-GAS GUN PERFORMANCE by W. B. Stephenson, May 1961. 49 pp. (ARO Project No. 386079) (AFSC Program Area 750A, Project No. 8950, Task 89600) (AEDC-TR-61-1) (Contract No. AF 40(600)-800 S/A 11(60-110)). Unclassified

7 references

One-dimensional, unsteady flow theory of an ideal gas is reviewed as it applies to guns and ballistic model launchers. The method of characteristics is developed for the general case including chambrage and finite chamber volume. Results for helium as a propellant are given from which the required chamber size can be determined. The launch velocity for combinations of launch tube and chamber geometries is computed assuming no friction nor heat loss and an evacuated bore.

1. Hypervelocity guns
2. Aeroballistics
3. Light-gas guns--Performance--Theory
4. Gas flow--Theory
5. Helium
I. Stephenson, W. B.

UNCLASSIFIED